Journal of Hazardous Materials 417 (2021) 125960

Contents lists available at ScienceDirect

Journal of Hazardous Materials

journal homepage: www.elsevier.com/locate/jhazmat

Review

Recent advances in the polyurethane-based adsorbents for the decontamination of hazardous wastewater pollutants

Rangabhashiyam Selvasembian [a,*], Willis Gwenzi [b,*], Nhamo Chaukura [c], Siyanda Mthembu [c]

[a] Department of Biotechnology, School of Chemical and Biotechnology, SASTRA Deemed University, Thanjavur 613401, Tamilnadu, India
[b] Biosystems and Environmental Engineering Research Group, Department of Soil Science and Agricultural Engineering, Faculty of Agriculture, University of Zimbabwe, P. O. Box MP 167, Mount Pleasant, Harare, Zimbabwe
[c] Department of Physical and Earth Sciences, Sol Plaatje University, Kimberley, South Africa

ARTICLE INFO

Editor: Dr. H. Artuto

Keywords:
Adsorption
Polyurethane
Removal mechanisms
Regeneration
Water pollutants

ABSTRACT

The pollution of aquatic systems with noxious organic and inorganic contaminants is a challenging problem faced by most countries. Water bodies are contaminated with diverse inorganic and organic pollutants originating from various diffuse and point sources, including industrial sectors, agricultural practices, and domestic wastes. Such hazardous water pollutants tend to accumulate in the environmental media including living organisms, thereby posing significant environmental health risks. Therefore, the remediation of wastewater pollutants is a priority. Adsorption is considered as the most efficient technique for the removal of pollutants in aqueous systems, and the deployment of suitable adsorbents plays a vital role for the sustainable application of the technique. The present review gives an overview of polyurethane foam (PUF) as an adsorbent, the synthesis approaches of polyurethane, and characterization aspects. Further emphasis is on the preparation of the various forms of polyurethane adsorbents, and their potential application in the removal of various challenging water pollutants. The removal mechanisms, including adsorption kinetics, isotherms, thermodynamics, and electrostatic and hydrophobic interactions between polyurethane adsorbents and pollutants are discussed. In addition, regeneration, recycling and disposal of spent polyurethane adsorbents are reported. Finally, key knowledge gaps on synthesis, characterization, industrial applications, life cycle analysis, and potential health risks of polyurethane adsorbents are discussed.

1. Introduction

Contamination in water bodies arises due to various environmental pollutants from natural and anthropogenic activities of industrial sectors, domestic activities, agricultural practices, global changes, etc. Worldwide, the toxicity of pollutants imposes negative effects because of their hazardous effects on living systems, food chains, deterioration of economy and environment (Hanieh et al., 2021; Hariharan et al., 2020; Mustapha et al., 2019). The desired characteristics of water quality are declining constantly because of adverse chemical releases. The predominant pollutants occurring in the water bodies include various types of organic pollutants and inorganic pollutants emanating from point and non-point sources (Faysal et al., 2020; Rangabhashiyam and Vijayaraghavan, 2019; Selvakumar and Rangabhashiyam, 2019; Tahir et al., 2020). Fig. 1 illustrates the different forms of water pollutants released from industrial effluents. Wastewater is laden with different chemicals of organic and inorganic origin (Dixit et al., 2011). Toxic heavy metal ions belong to the inorganic pollutant type of the trace elements with elemental density greater than 4 ± 1 g/cm^3. Anthropogenic activities such as electroplating, fertilizers, batteries, photography, landfills, mining contribute to the heavy metal contamination in the water bodies (Khan et al., 2021; Viraj et al., 2020). Even though at the trace concentration metal ions are generally beneficial for biological activities, they nevertheless exhibit harmful effects when the concentrations exceed the permissible concentrations (Jessica et al., 2020; Radha et al., 2019). Synthetic dyes find application in different industries including textile, paper and pulp, printing, food production, paint, leather tanning, plastic, cosmetics, rubber, etc. Dyes consist of complex molecular structure, resist biodegradation, and exhibit stable characteristics (Ali et al., 2020; Magdalena and Marieta, 2018; Tan et al., 2016; Dutta et al.,

* Corresponding authors.
E-mail addresses: rangabhashiyam@scbt.sastra.edu (R. Selvasembian), wgwenzi@agric.uz.ac.zw, wgwenzi@yahoo.co.uk (W. Gwenzi), nhamo.chaukura@spu.ac.za (N. Chaukura), siyanda.mthembu@spu.ac.za (S. Mthembu).

https://doi.org/10.1016/j.jhazmat.2021.125960
Received 22 January 2021; Received in revised form 18 April 2021; Accepted 21 April 2021
Available online 5 May 2021

2020). The occurrence of dyestuff even at low concentrations of less than 1 mg/L in water bodies affects the esthetic property, transparency of water and interfere with photosynthesis due to absorption and reflection of sunlight entering water bodies (Subramanian et al., 2018; Zonoozi et al., 2015). Practical uses of pesticides occurs in different forms such as herbicides, insecticides, bactericides, fungicides, virucides, etc based on the specific purpose to protect the ecosystem and prevention of disease transmission (Foo and Hameed, 2010). Pesticides usage has been reported as lethal to human beings and affects environment. Prolonged exposure to certain herbicides causes cardiovascular damage, carcinogenic effects, liver problems, anemia, toxicity to fresh water fish, and affects plant photosynthesis (Iman et al., 2020; Esperanza et al., 2019). The main source of pharmaceuticals in water bodies are domestic, hospital, and pharmaceutical effluents (Hugo et al., 2021). The consumption of different pharmaceutical compounds has constantly increased over the years. The utilization of pharmaceuticals compounds spiked about 24% during the last five years with worldwide 4500 billion doses (Quintiles IMS, 2015). Consequently, pharmaceuticals are widely distributed in ground water and surface water varying in the concentrations of a few ng/L to several hundred μg/L. The ecological health risks of pharmaceuticals include the proliferation of bacterial strains resistant to antimicrobial agents, neurotoxicity, genotoxic, mutagenic, fetotoxic, endocrine disruption, and metabolisms disruptions (Zeng et al., 2018; Raphael et al., 2017; Moreira et al., 2016). Oily wastewaters are generated from oil refining during fuel production. Particularly, the process of extraction forms the oil/water mixtures of about 50 million m^3/day, salinity range of 0–300,000 mg-TDS/L and distribution of oil in water greater than 500 mg/L (Ahmad et al., 2016). Wastewaters generated from petroleum refinery are laden with various compounds of aromatic and aliphatic hydrocarbons. Because it is characteristically immiscible with water, oil forms a distinct layer on the water bodies, prevents sunlight penetration and gaseous exchange, resulting in oxygen stress and ultimately death of aquatic organisms. Prolonged human exposure to oil containing hydrocarbons causes severe health hazards (Saad et al., 2019; Mahak et al., 2020).

Various research groups, government and non-government agencies are working on water pollution abatement globally for the conservation of water resources. The worldwide distribution of population is predicted to reach about 9.3 billion by 2050, and under such circumstances the world population may be under great fresh water scarcity (United Nations, 2011). Owing to the priority of water requirements in life, proper treatment approaches for the enhancement of water quality and water resource preservation are required. In this review, the research output based on the keyword search of wastewater pollutants treatment from the Scopus database showed a total 39,662 articles published from 1969 to 2020. Fig. 2 indicates the Scopus extracted data with the analysis results in the form of documents type, subject area, country/territory, and year of publication. The results analysis revealed increased interest among researchers on the treatment of wastewater towards pollutant elimination from the water bodies.

2. Water pollutants remediation approaches

The removal of pollutants present in the wastewater takes place by means of different technologies (Fig. 3) including membrane filtration, ion-exchange, chemical precipitation, solvent extraction, electrochemical conversion, oxidation, reverse osmosis, ozonation, photocatalysis, coagulation, incineration, adsorption, and biological degradation (Abdelrahman et al., 2020; Sarode et al., 2019; Torres et al., 2011). The conventional treatment of wastewater pollutants through activated sludge and biological filtration presents lesser performance efficiency in terms of contaminant removal (Tran et al., 2017). Chemical precipitation, advanced chemical oxidation, and membrane based separation methods are limited by the requirements of high cost investments and complex processes. Further, high costs factors in optimization of the treatment process, generation of hazardous wastes after treatment, less flexibility for treatment of multi-component pollutants, and more energy demands hinder the process development and implementation for the large scale applications (Sarode et al., 2019; Georgescu et al., 2018). Adsorption refers to the accumulation of a solute at a surface or in the interfacial region of the adsorbent. Pollutant removal in wastewater treatment via adsorption is thus carried out at an interfacial region between adsorbent and the pollutant. Compared to other methods for remediation of contaminants in aqueous systems, adsorption has the advantages of low cost, simple design, efficient and eco-friendliness. A range of adsorbents have been developed from various sources and used for the remediation of contaminants in the wastewater. For example, the adsorption process has been carried out using native forms of materials, activated carbon prepared from lignocellulosic biomass, industrial wastes, biological wastes, chemically synthesized adsorbents, and natural resources (Sarita et al., 2019; Rangabhashiyam and Balasubramanian, 2018; Maryam and Mohammad, 2020; Rangabhashiyam and Balasubramanian, 2019; Vikash and Vimal, 2020; Zahra and Ali, 2019; Yuling et al., 2021; Xin et al., 2020). Other treatment of wastewater using the physico-chemical methods involve the costs range of 10–450 US$/$m^3$ water treated, whereas the cost of water treatment through adsorption was 5.0–200 US$/$m^3$ (Gupta et al., 2012). Moreover, the adsorption process successfully reported the elimination of multi-component pollutants distributed in the wastewater. The removal of contaminants in wastewater is influenced by the process parameters including solution pH, contact time, initial pollutant concentration, adsorbent dosage, temperature, and concentration of co-existing ions (Manjunath and Kumar, 2018; Hanandeh et al., 2021; Akeem and Mustafa, 2015). Further, the investigation of pollutant

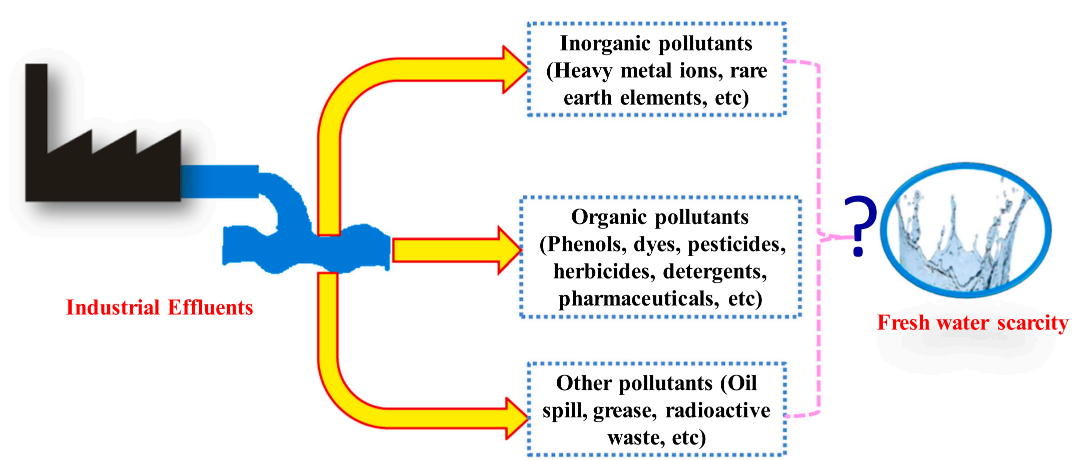

Fig. 1. Various forms of water pollutants from industrial effluents.

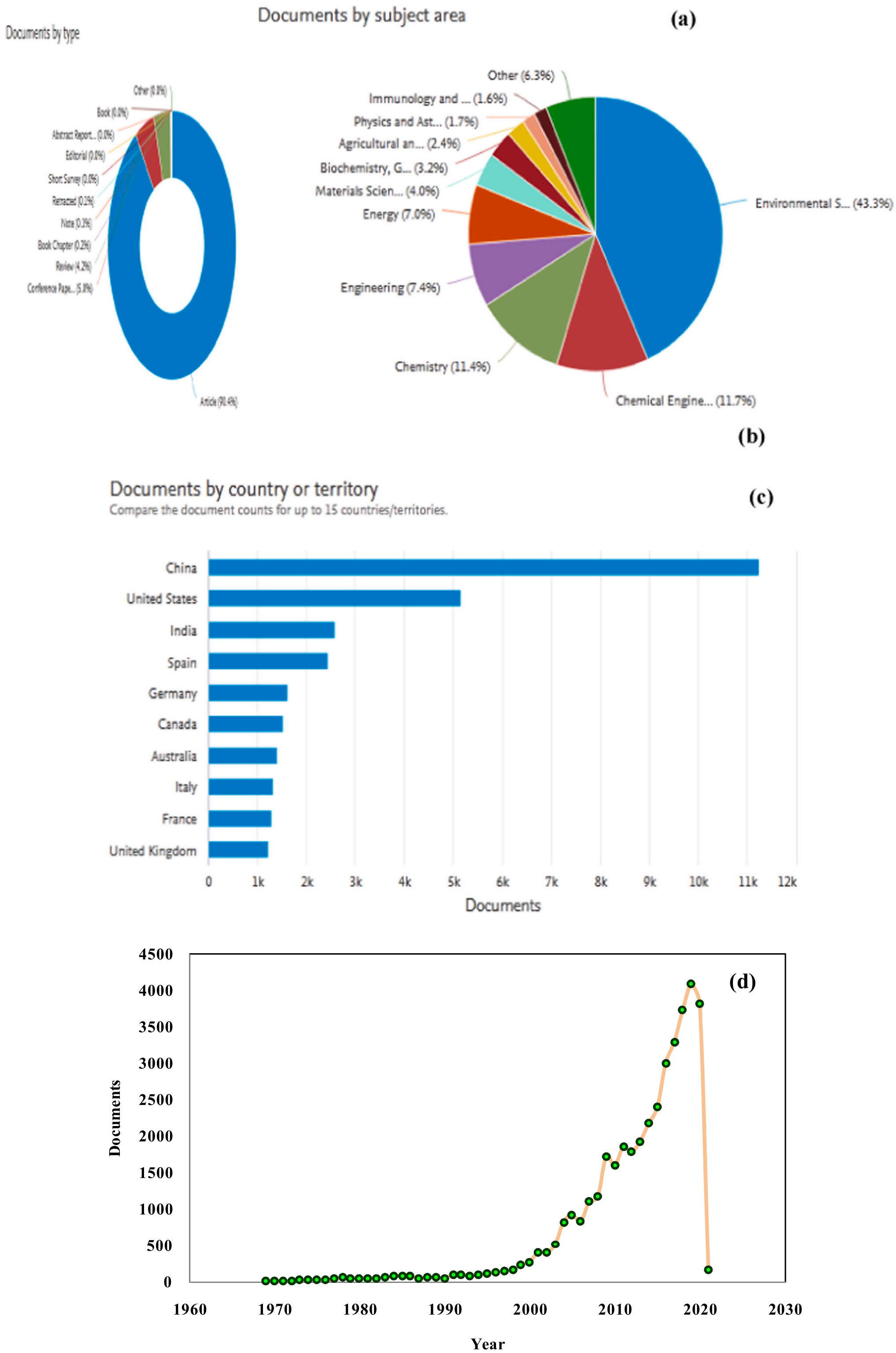

Fig. 2. Scopus extracted data for the keyword search for wastewater pollutants treatment up to 2020, by (a) documents type, (b) documents subject area, (c) source country/territory, and (d) documents.

removal using batch systems followed by continuous adsorption studies is important for understanding the potential for commercial scale application. The continuous adsorption process involves the parametric analysis of initial pollutant concentration, adsorbent bed height, influent flow rate and pH of influent (Rangabhashiyam et al., 2016; Igberase and Osifo, 2019). Research related to the used of the adsorption method for the remediation of various contaminants in wastewater have shown an increasing trend according to the data extracted from Scopus (Fig. 4).

3. Preparation of polyurethane

Polyurethane is a polymer composed of the carbamate groups in its structure resulting from the reaction between isocyanate and polyol

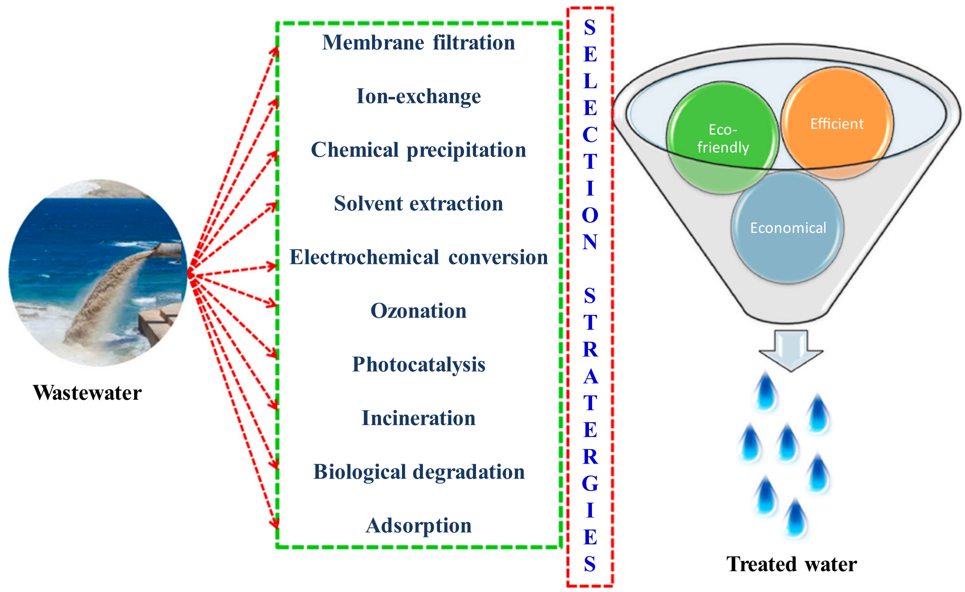

Fig. 3. Wastewater treatment methods.

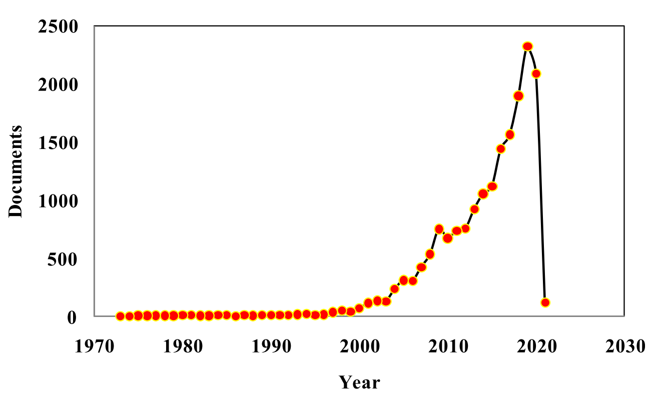

Fig. 4. Scopus extracted data for the keyword search for adsorption and water pollutants removal up to 2020.

moieties. A number of methods exist for the preparation of polyurethane foam (PUF), which is subsequently used as a precursor for the development of polyurethane based adsorbents for the remediation of contaminants in aqueous systems. Generally, the synthesis of polyurethane involves the polymerization reaction between diisocyanates and polyols with or without the use of a catalyst, a blowing agent, and surfactant. The polymerization reaction can be base, acid or polyol-catalyzed synthesis. The prepolymer is modified by reacting the terminal iisocyanate groups with various adsorbents to form the final polyurethane foam. The choice of diisocyantes and polyols gives the PUF its characteristic hard and soft domains. The carbamate group is the urethane linkage (–NHOCO–), and it occurs in the form of a repetitive units.

3.1. *Polymerization reaction mechanism*

The general classifications of the polyurethanes includes the types of AA–BB and A–B. The polyurethane type of AA–BB prepared by means of the addition of diols to diisocyanates and another type of polyurethane A–B through the α, ω-isocyanate alcohols self-addition (Fernández et al., 2010).

3.1.1. *Base catalyzed reactions*

The base catalyzed reaction mechanism uses catalysts like 1,4-diazabicyclo[2.2.2]octane (DABCO) (Sonnenschein and Wendt, 2013.), 1,5,7-triazabicyclo[4.4.0]dec-5-ene (TBD), *N*-methyl-1,5,7-triazabicyclododecene (MTBD), 1,8-diazabicyclo[5.4.0]undec-7-ene (DBU) (Kaljurand et al., 2000, 2005), N-heterocyclic carbenes and 1, 3-bis(ditertiobutyl)imidazol-2-ylidene (Coutelier et al., 2012.). The base catalyst may nucleophilically add to the carbonyl of isocyanate group generating an oxide (Fig. 5a [i]). The oxide then tautomerizes to a nitride regenerating the carbonyl group. The nucleophilic addition of oxygen atom to the polyol of the carbonyl group leads to a five membered transition state. The carbonyl group is subsequently regenerated eliminating the base catalyst followed by the protonation of the nitrogen by the proton from the incoming polyol (Baker and Haldsworth, 1947; Baker et al., 1949; Burkus, 1961).

Recently, Sardon et al. (2013) have described a base catalyzed reaction mechanism where the oxygen atom from polyol is activated owing to hydrogen bonding between the base and hydrogen atom of the hydroxyl group (Fig. 5a [ii]). The oxygen of the polyol then nucleophilically add to the carbonyl carbon of the isocyanate group leading to a nitride. The nitride is then protonated by the hydrogen from the OH group of the polyol to achieve the desired PU.

3.1.2. *Acid-catalyzed reactions*

The acid catalyzed reaction mechanism uses catalyst like triflic acid, trifluoromethanesulfonimide (Kutt et al., 2010), methanesulfonic acid, p-toluene sulfonic acid and diphenylphosphate (Coady et al., 2013; Sardon et al., 2013). The oxygen atom on the isocyanate group is protonated followed by the nucleophilic addition of OH to the carbonyl carbon (Fig. 5b [i]). The nitrogen atom is then protonated by the proton of the incoming alcohol. Ultimately, the carbonyl group reforms generating the acid catalyst and breaking the imine double bond resulting in a carbamic ester (Sardon et al., 2013).

Alternatively, the nitrogen atom of the isocyanate group may be activated by protonation with an acidic proton, followed by nucleophilic addition of the hydroxyl group to the carbonyl carbon of the isocyanate group (Fig. 5b [ii]). The resulting intermediate then rearranges to generate the PU and the acidic proton (Sardon et al., 2013).

3.1.3. *Polyol-catalyzed polymerization reaction*

The polyol catalyzed reaction uses one OH group as a catalyst for another OH group reacting with an NCO group. The oxygen atom of the first OH group undergoes nucleophilic addition to the carbonyl carbon of the NCO group resulting in an oxide, which subsequently tautomerizes into a nitride (Fig. 5c). The oxygen atom of the second OH group

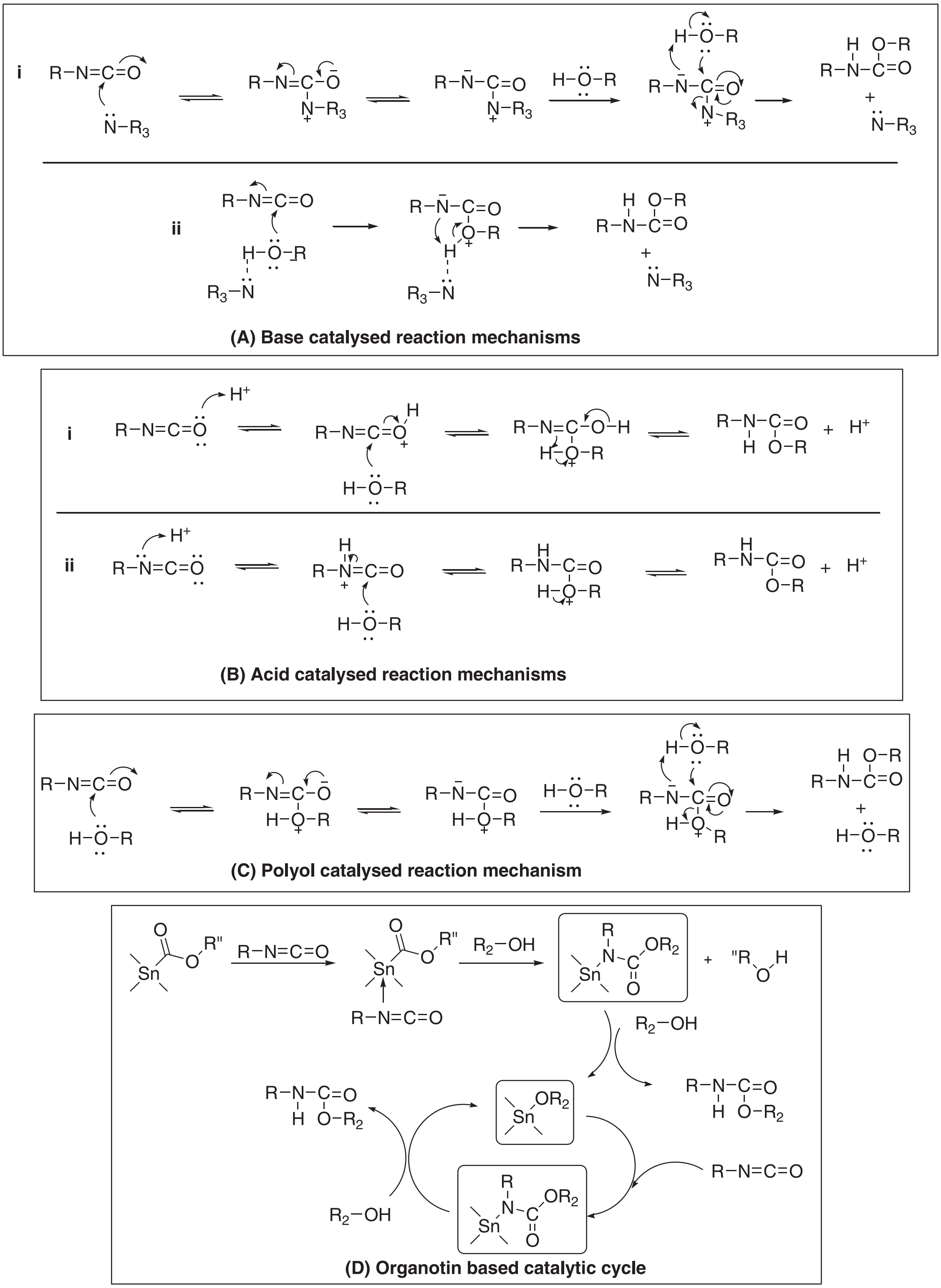

Fig. 5. Possible reaction mechanisms for base, acid, and polyol-catalyzed synthesis of polyurethane. Based on extracts (Baker and Haldsworth, 1947; Baker et al., 1949; Burkus, J., 1961; Sardon et al., 2013; Fisch and Rumao, 1970; Raspoet et al., 1998).

nucleophilically adds to the carbonyl carbon accompanied by the elimination of the first OH group followed by protonation of the nitride by the proton of the second OH group. This leads to the formation of a carbamic ester (Fisch and Rumao, 1970; Raspoet et al., 1998).

3.1.4. *Organotin based catalytic cycle*

The organotin catalytic cycle uses catalyst like dibutyltin dilaurate and dibutyltin diacetate. Bloodworth and Davies proposed that the catalytic cycle involves the formation of N-stannylurethane by a reaction nitrogen-tin coordinated compound with alcohol (Fig. 5d). The stannylurethane undergoes further alcoholysis to achieve targeted urethane and tin alkoxide which starts the catalytic cycle. Isocyanate then add to tin alkoxide resulting in stannylurethane, which undergoes alcoholysis to produce the targeted urethane and tin alkoxide.

Overall, preparation methods for PUF should be evaluated based on the cost and how rapid the reaction kinetics occur. This will in turn influence the use of the synthesis method at a large scale. In this regard, base-catalyzed and acid-catalyzed preparation methods are preferable owing to their simplicity and rapid kinetics.

3.2. The influence of preparation method on properties of PUF

The characteristics of PUF include good mechanical strength, resistance to oxidation, chemical stability, and good elasticity (Khalid et al., 2007; Misbah et al., 2012). The occurrence of soft and hard domains influences the characteristics (soft, flexible or hard) of the final product. The soft segments are predominantly the longer chain polyols and diols, and confer mobility and flexibility to the polyurethane. Whereas the hard segments emanate from the usage of isocyanates and chain extender. Isocyanates are commonly short chain, which cause more crystallization and result in rigid structures. Such a mixture of both hard and soft domains produces polyurethane with characteristics potentially useful in a range of applications. The rigidity of the polyurethane based products is mainly from the intrinsic interaction of short chains and urethane groups through cross-linking. Furthermore, polyols containing lengthy stretchy chain segments are another important component in the formation of polyurethane. Apart from isocyanate and polyols, the other components of polyurethane formulations include catalysts, plasticizers, pigments, cross-linkers/chain extenders, blowing agents and surfactants, fillers and flame retardants. The variation in the precursors of isocyanate and polyols creates the different forms of polyurethane with distinct properties (Abhijit and Prakash, 2020; Fernández et al., 2010; Sultan et al., 2015; Lin et al., 2019). The polyurethane types of foamed plastics, elastomers, coatings, adhesives, sealants, leather resins and waterproof materials find wider applications in building and construction, transport, textile, footwear, clothing, furniture, glass, electronics, appliances, foundry, packaging, among others. Polyethylene glycol, polyethylene oxide, polypropylene glycol, polytetramethylene glycol represent different forms of polyurethane based industrial products (Akindoyo et al., 2016; Waletzko et al., 2009). Blow molding introduces voids in the polymer. Such voids present excellent characteristics of mechanical properties, permeability, elasticity, hydrophobicity high porosity, flexibility, low density, chemical resistance etc (Larissa et al., 2020; Santos et al., 2017). Polyurethane is also flexible and suitable for regeneration for reuse through mechanical post-treatment approaches (Simon et al., 2018; Zia et al., 2007). Different routes of the recycling of polyurethane are illustrated in Fig. 6.

Fig. 6. Outline of polyurethane recycling.

4. Preparation of functionalized PUF adsorbents

Modification of PUF through the incorporation of various additives increases hydrophobicity (Anju and Renuka, 2020; Khalilifard and Javadian, 2020; Guselnikova et al., 2020), surface area (Khalilifard and Javadian, 2020), selectivity (Jamsaz and Goharshadi, 2020; Sone et al., 2009), hydrogen bonding (Kumari et al., 2016) and ionic bonding (Yang et al., 2013; Eibagi et al., 2020), ion-dipole interaction (Khan et al., 2015; Kalaivani et al., 2016; Ranote et al., 2019) and thus improves the contaminant adsorption capacity (Xue et al., 2019; Anju and Renuka, 2020; Khalilifard and Javadian, 2020; Guselnikova et al., 2020). The extent to which the performance is enhanced largely depends on the modification process and chemistry of the various components included in the PUF matrix. Commercially available PUFs have been modified by grafting additives on the surface of the polymers by means of chemical and physical adhesion. Functionalized PUF adsorbents used for decontamination include: (1) clay-PUF composites, (2) chitosan-PUF composites, (3) carbon-modified PUFs, (4) PUF-metal oxide composites, (5) alginate-PUF composites, (6) graphene-PUF composites, and microbes immobilized on PUF. The development of nanotechnology has opened new opportunities for advanced modification using nanostructured materials such as carbon nanotubes and metal oxide nanoparticles (Noorisafa et al., 2016). Such modifications can be tailored to remove specific pollutants. Owing to their photocatalytic properties, metal oxide nanomaterials present the advantage of photodegrading the adsorbed pollutants, resulting in a self-cleaning adsorbent. Modification with nanoparticles increases the specific surface area and the overall surface functionalities, and subsequently improve the adsorptive performance of PUF. In addition, antimicrobial activity can be conferred through modification with compounds derived from chlorohydroxy-furanone (Xie et al., 2018). Such properties are desirable in prolonging the lifespan of the adsorbent. Here, a summary of the preparation and intended applications is summarized. Table 1 presents the materials used for the preparation of various PUF adsorbents reported in literature.

4.1. Clay-PUF composites

Clay nano-adsorbents have been used to modify polyurethane to control surface properties. For example, these have been synthesized by a reaction between 4,4′-methylene bisphenyl diisocyanate, 1,4-butanediol, polytetramethylene oxide and low level *N*,*N*′-ethylenebisstearamide, followed by melt-blending with clay nanoparticles (Lyu et al., 2007). In another study, an open cell PUF modified with nanoclay were synthesized by reacting polyether polyol dispersed in nanoclay with methylene diphenyl diisocyanate using 1,2-dichloro-1-fluoroethane as a surfactant and deionized water as the blowing agent (Nikkhah et al., 2015). A similar study synthesized zeolite, activated carbons, and pillared clay supported on open cell PUF by reacting polymeric 4,4′-methylene bisphenyl diisocyantate and tris(polyoxypropylene ether)propane in the presence of dibutyltin dilaurate catalyst followed by the addition of zeolite, activated carbon, pillared clay in separate reactions in the presence of silicone oil and water as surfactant and blowing agent, respectively (Pinto et al., 2005).

4.2. Chitosan-PUF composites

A PUF was synthesized by reacting toluene diisocyanate and polyol polyether that has a 2,4 and 2,6 isomers in the ratio 8:2 (Centenaro et al., 2017). The resulting PUF was then coated with chitosan and used in the remediation of contaminated effluent. In another study, a polyethylene glycol-based PUF modified with chitosan with different molecular

Table 1
Summary of materials used for the preparation of various polyurethane (PUF) adsorbents reported in literature.

POLYMER	DIISOCYANATE/ PUF / PREPOLYMER	POLYOL	ADDITIVES	CATALYST	BLOWING AGENT	SURFACTANT	REACTION TYPE	REFERENCE
Clay-PUF composites								
Clay nano-adsorbants modified polyurathane	4,4′-methylene bisphenyl diisocyanate	1,4-butanediol	Polytetramethylene oxide, N,N′-ethylenebisstearamide (hydrophobic additive), clay fillers				One shot	Lyu et al., 2007
Open cell Polyurethane foam modified with nanoclay	Methylene diphenyl diisocyanate	Polyether polyol	Nanoclay		Deionized water	1,2-Dichloro-1fluoroethane		Nikkhah et al., 2015
Zeolite, activated carbons, and pillared clay supported on open cell polyurethane foams	Polymeric 4,4′-methylene bisphenyl diisocyantate	Tris(polyoxypropylene ether)propane	Zeolite (NaX), activated carbon, pillared clay	Dibutyltin dilaurate	water	Silicone oil		Pinto et al., 2005
Chitosan-PUF composites								
Chitosan-coated Polyurethane foam	Toluene diisocyanate	Polyol polyether(2,4 and 2,6 isomers; 8:2 ration)	Chitosan					Machado Centenaro et al., 2017
Polyethylene glycol-based polyurethane foams modified by chitosan	Poly(ethylene glycol	Isophorone diisocyanate	Chitosan, D-glucosamine	Tin bis(2-ethylhexanoate)	triethylenediame	Silicone oil	Two step method	(Qin and Wang, 2019)
Bio-based polyurethane composite	Hexamethylene diisocyanate biuret	Chitosan and glutaraldehyde (crosslinked)	Ricinoleic acid				One-shot	da Rosa Schio et al., 2019
Carbon modified PUFs and nanotube-PUF composites								
Multiwalled carbon nanotube-polyurethane composite	Toluene diisocyantate	Castor oil	Multiwalled carbon nanotubes					Khan et al., 2015
Polyurethane foam adsorbent modified with coal	Isophoronediisocyanate	Polyether polyol	Pulverized coal	Dibutyltin dilaurate	Sodium bicarbonate	Silicone oil	One step method	Kong et al., 2016
Algae-based polyurethane film	4,4′-methylene diphenyl diisocyanate	Algae polyol particles (Genus: Chaetomorpha; Family: Cladophoraceae; Class: Ulvophyceae	Activated carbon					Marlina et al., 2020
Novel Cellulose Nanowhiskers-poylurathene foam	4,4′-diphenylmethane diisocyanate	Cellulose nanowhiskers		Triethy amine, triethanolamine (co-catalyst)	Distilled water	Silicone oil		Kumari et al., 2016
Pine cone biomass cross-linked polyurathane	Hexamethylene diisocyanate	Pine cone biomass (Fenton's pre-treated)		Dibutyltin dilaurate				Kupeta et al., 2018
Hydrophobic polyurethane/castor oil biocomposite with agroindustrial residues	Methylene diphenyl diisocyanate	Castor oil	Bagasse malt; Acerola residue				Two step method	Amorim et al., 2021
Moringa oleifera gum-based biofunctional polyurethane	4,4′-diphenylmethane diisocyanate	Moringa gum (purified)	Ash	1,4-diazabicyclo[2.2.2]octane (co-catalyst)	Distilled water	Silicone oil		Ranote et al., 2019
	p-styrenesulfonate			Ammonium persulfate	Deionized water			Jin et al., 2020

(*continued on next page*)

Table 1 (*continued*)

POLYMER	DIISOCYANATE/ PUF / PREPOLYMER	POLYOL	ADDITIVES	CATALYST	BLOWING AGENT	SURFACTANT	REACTION TYPE	REFERENCE
Functionalised polyurathane sponge based on dopamine		N-(3,4-dihydroxyphennethyl) acrylamine					In situ polymerization	
Hyper branched polyurethane resins	4,4′-methylene bis(phenyl isocyanate)	(E)-4-((4-hydroxyphenylimino) methyl)benzene-1,2-diol						Kalaivani et al., 2016
	Toluene diisocyanate	Polypropylene glycol; Polypropylene glycol and p-tert-butylacalix[4] arene		1,4-diazabicyclo[2.2.2]octane; Dibutyltin dilaurate	Distilled water		One shot method	Mohammadi et al., 2014
Linear and crosslinked polyurethanes	Toluene diisocyanate	Polyethylene glycol; Polyethylene glycol and tetraethyl pentamine (crosslinker)			Distilled water			(Sultan et al., 2018)
A linear and crosslinked polyurethanes	Hexamethylene diisocyanate	Poly (tetramethylene ether) glycol; 1,4-butanediol		AIBN			Two step method	Zenoozi et al., 2020
Polyurethane/palm fiber biocomposite	4,4′-diphenylmethane diisocynate and castor oil (NCO terminated)		Palm fiber				Chain extension reaction	Martins et al., 2020
Carboxymethlyated cellulose nanofibrils embedded polyurethane foams	HYPOL™ JT6000 (NH_2 terminated by reaction with water)		Carboxymethlyated cellulose nanofibrils					Hong et al., 2018
Polyurethane/ sepiolite cellular nanocomposites			Sepiolite clay (Hydrated magnesium silicates)		Distilled water	Polyether-polydimethylsiloxane-copolymer		Barroso-Solares et al., 2020
Carbon media functionalized Polydopamine-coated open cell polyurethane foam	Open cell polyurethane foam; Carbon media functionalized Polydopamine-coated open cell polyurethane foam		Polydopamine, Activated carbon/ carbon nanotubes (acid functionalized); Activated carbon/ carbon nanotubes (Increase the mass of the carbon media)					Lefebvre et al., 2018
Dithioic acid functionalized polyurethane foam	Commercial		Carbon disulfide					Yang et al., 2013
Superhydrophobic polyurethane sponge modified by seashell	Commercial		Calcined seashell powder					Jamsaz and Goharshadi, 2020
Polyaniline nanoparticles mobilized polyurethane	Waste of furniture		Aniline	Ammonium persulfate				Vali et al., 2018
Prussian blue and amylopectin impregnated polyurethane sponge	Commercial		Prussian blue nanocubes and amylopectin					(Zhuang et al., 2016)
Nanochitosan and polypropylene glycol blended polyurethane	Commercial		Nano chitosan, polypropylene glycol	Glutaraldehyde (crosslinking agent)				Saranya et al., 2017

(*continued on next page*)

Table 1 (*continued*)

POLYMER	DIISOCYANATE/ PUF / PREPOLYMER	POLYOL	ADDITIVES	CATALYST	BLOWING AGENT	SURFACTANT	REACTION TYPE	REFERENCE
PUF-metal/metal oxide composites								
Open cell Polyurathane foam nanocomposite	Toluene diisocyanate	Polypropylene glycol	Iron oxide nanoparticles		Deionized water, CO_2	polysiloxane		(Hussein and Abu-Zahra, 2016)
β-cyclodextrin poly (urethane-imide) grafted onto magnetic nanoparticles	5-isocynato-2-(4-isocyanatophenyl) isoindoline-1,3-dione (syntheized)	β-Cylodetrin	Iron oxide nano particles (prepared) No nano particles				(a) One shot (b) Surface grafting	Eibagi et al., 2020
Magnetic superhydrophobic PU-$(CF_3)_2$-FeNPs-$(CF_3)_2$	Commercial		3,5-bis(trifluoromethyl) benzenediazonium tosylate (ADT-$(CF_3)_2$); FeNPs-($(CF_3)_2$					Guselnikova et al., 2020
Silver functionalized Polydopamine-coated open cell polyurethane foam	Polydopamine-coated open cell polyurethane foam		Silver Nitrate					Lefebvre et al., 2017
Indolocarbazole based polymer coated polyurethane sponge	Commercial		ICZP6 polymer (prepared from 9,9-diocyl-2,7-diethynyfluorene and 2,8-dibromoindolo[3,2-b]carbazole monomers); ICZP6 polymer and iron oxide					Vintu and Unnikrishnan, 2019
Alginate-PUF composites								
Alginate/ Polyurethane foams	Poly(oxy C2–4 alkylene) diol and toluene diisocynate (NCO terminated)	Sodium alginate				Poly(ethylene oxide)-block-poly(propylene oxide)-block-poly (ethylene oxide)		Sone et al., 2009
Graphene-PUF composites								
Poly-Cys-g-PDA@GPUF	Polyether 100% open cell (NH_2 terminated modification)		Graphene oxide; Polydopamine; Cysteine methacrylate monomer					Xue et al., 2019
Graphene/Iron oxide, Graphene oxide and Iron oxide coated polyurethane foams	Commercial		Graphene oxide; Iron oxide; Ascorbic acid					(Anju and Renuka, 2020)
Polyurethane sponge loaded with Fe_3O_4@oleic acid@graphene oxide	Commercial		Iron oxide, oleic acid, graphene oxide nanosheets					Khalilifard and Javadian, 2020
Microbe-impregnated PUFs								
Nitrifying sludge immobilized waterborne polyurethane pellets	Waterborne polyurathane		Nitrifying sludge (purified by deionized water and phosphate buffer saline)	Tetramethylethylenediamine and potassium persulfate (initiators)				(Lu et al., 2019)

weights was synthesized by in two steps (Qin and Wang, 2019). The prepolymer was first prepared in a reaction between poly(ethylene) glycol and isophorone diisocyanate followed by the foam reaction of the prepolymer with D-glucosamine and chitosan, respectively, in the presence catalytic tin bis(2-ethylhexanoate), triethylenediame as a blowing agent and silicon oil as a surfactant. Chitosan has also been used as a polyol in the preparation of bio-based chitosan/PUF composite foam, where a solution of glutaraldehyde cross-linked with chitosan was reacted with mixture of hexamethylene diisocyanate and ricinoleic acid (da Rosa Schio et al., 2019). Overall, incorporating chitosan into the PUF matrix enhanced the physico-chemical and subsequently the pollutant removal properties of the foam.

4.3. Carbon modified PUFs and nanotube-PUF composites

A multi-walled carbon nanotube-polyurethane composite was synthesized by reacting castor oil and toluene diisocyanate followed by adding oxidized carbon nanotubes to the newly formed prepolymer (Khan et al., 2015). In another study, Brilliant green was removed using a PUF modified with coal in a reaction involving isophoronediisocyanate, polyether polyol and pulverized coal (Kong et al., 2016). An algae/activated carbon-based polyurethane film for the removal of NH_3–N has been synthesized via a reaction between 4, 4′-methylene diphenyl diisocyanate and ball mill pretreated algae polyol particles to form PUF (Marlina et al., 2020). Activated carbon fillers were then added to the resulting PU.

Novel cellulose nanowhisker-based polyurethanes have been synthesized in a reaction between cellulose nanowhiskers as polyol, and 4,4′-diphenylmethane diisocyanate (Kumari et al., 2016). In the reaction, trimethylamine and triethanolamine were used as co-catalysts, while silicone oils and distilled water were used as a surfactant and blowing agent, respectively (Kumari et al., 2016). In a separate study, a PUF adsorbent was synthesized by reacting a pine cone biomass pretreated with Fenton's reagent pretreated as a polyol with hexamethylene diisocyanate in the presence of dibutyltin dilaurate (Kupeta et al., 2018). The prepared PUF adsorbent was used in a kinetic and equilibrium adsorption study of 2-nitrophenol (Kupeta et al., 2018). Other researchers have developed a hydrophobic castor oil/PUF biocomposites incorporating agro-processing residues for the adsorption of organic solvents and oils (Amorim et al., 2021). They synthesized the PUF/castor oil foams (PUCO) and biocomposites by polymerizing methylene diphenyl diisocyanate (prepolymer) and polyol in a 1:1 ratio in a one-shot free expansion method. Ricinoleic acid was used to increase the hydrophobicity of the PUCO foam. In the same study, the agro-processing residues were grafted individually using mix proportions of 5%, 10%, 15% and 20% (Amorim et al., 2021). The connection between the polymer and the agro-processing residues occurred in a reaction involving free NCO groups and the OH groups of the residues. A *Moringa oleifera* gum-based biofunctional PUF loaded with ash have been synthesized for rapid and efficient removal of dye (Ranote et al., 2019). Purified *Moringa oleifera* gum (MOG) was reacted with 4,4′-diphenylmethane diisocyanate to form MOG-PUF using the following; (1) 1,4-diazabicyclo[2.2.2]octane as a co-catalyst, (2) ash as a filler, (3) silicone oils as a surfactant, and (4) water as a blowing agent.

In another study, dopamine-based PUF was synthesized by reacting N-(3,4-dihydroxyphennethyl) acrylamine with p-styrenesulfonate in an in situ polymerization reaction (in a polyurethane sponge) in the presence of ammonium persulfate catalyst (Jin et al., 2020). The reaction between 4,4′-methylene bis(phenyl isocyanate) and (*E*)-4-((4-hydroxyphenylimino)methyl)benzene-1,2-diol was used to synthesize hyperbranched polyurethane resins (Kalaivani et al., 2016). A study reported flexible PUF imbedded with p-tert-butyl thiacalix[4]arene synthesized by reacting p-tert-butylacalix[4]arene as a polyol with toluene diisocyanate forming a prepolymer (Mohammadi et al., 2014). The prepolymer was then reacted with polypropylene glycol in the presence of dibutyltin dilaurate as catalyst, 1,4-diazabicyclo[2.2.2]octane as co-catalyst, distilled water as a blowing agent, and silicon oils as a surfactant.

Sultan et al. (2018) synthesized linear and crosslinked polyurethane based catalysts for the reduction of methylene blue in a reaction between toluene diisocyanate and polyethylene glycol in distilled water resulting in the linear PU, while the cross-linked PU was achieved in the presence of tetraethyl pentamine. In a separate study, biocompatible semi-interpenetrating polymer networks (semi-IPNs) were prepared using polyurethane and cross-linked poly(acrylic acid) by first synthesizing polyether-based PUFs followed by the synthesis and fabrication of polyurethane-polyacrylic acid semi-IPNs (PU-PAA semi-IPNs) (Zenoozi et al., 2020). Hexamethylene diisocyanate was reacted with poly(tetramethylene ether) glycol without a catalyst to make the prepolymer, which was then reacted with 1,4-butanediol resulting in the desired polyurethane. Various ratios of N′-hexane-1,6-dilbisprop-2-enamide and acrylic acid were reacted with PU in situ via free radical l cross-linking polymerization using AIBN as an initiator to produce PU-PAA semi-IPNs.

Other carbon-modified PUFs reported in literature and their applications include: (1) polyurethane/palm fiber biocomposites (Martins et al., 2020), (2) carboxymethlyated cellulose nanofibrils (CMCNF) embedded polyurethane foams (Hong et al., 2018) that serve as modular adsorbents of heavy metal ions, (3) nanocomposite polyurethane foams used for remediation of nitrates-polluted water (Barroso-Solares et al., 2020), (4) nanochitosan and polypropylene glycol functionalized polyurethane foam for the adsorption of lead (II) in aqueous systems (Saranya et al., 2017), (5) open cell polyurethane foams functionalized with activated carbon/ carbon nanotubes used for the adsorption of a dye (methylene blue) (Lefebvre et al., 2018), and (6) a dithioic acid functionalized PUF adsorbent for the adsorption of EDTA-Ni(II) and EDTA-Cu(II) from aqueous systems (Yang et al., 2013). Jamsaz and Goharshadi (2020) synthesized a superhydrophobic calcined seashell powder modified polyurethane sponge for oil/water separation, while Vali et al. (2018) synthesized polyaniline nanoparticles immobilized polyurethane for removal of mercury from contaminated waters. A three-dimensional magnet carbon framework was prepared from amylopectin-impregnated PUF and Prussian blue for the removal of lead (Zhuang et al., 2016).

4.4. PUF-metal/metal oxide composites

Introducing metals or metal oxides into the PUF structure enhances pollutant removal properties. In one study, the open cell polyurethane foam nanocomposite for arsenic removal from drinking water was synthesized by reacting toluene diisocyanate with polypropylene glycol and doping with iron oxide nanoparticles where deionized water acted as a blowing agent and polysiloxane as a surfactant leading to the open call structure (Hussein and Abu-Zahra, 2016). A recent study grafted β-cyclodextrin poly(urethane-imide)s onto iron oxide magnetic nanoparticles by reacting 5-isocynato-2-(4-isocyanatophenyl)isoindoline-1, 3-dione(syntheized), β-Cylodetrin and iron oxide magnetic nanoparticles in a one shot method (Eibagi et al., 2020).

In one study, PUF was introduced into a solution of 3,5-bis(trifluoromethyl)benzenediazonium tosylate (ADT-$(CF_3)_2$ in acetonitrile resulting in PU-ADT-$(CF_3)_2$ (Geselnikova et al., 2020). The PU-ADT-$(CF_3)_2$ sponge was then inserted into a dispersion of pre-synthesized iron oxide nanoparticles (FeNPs-$(CF_3)_2$) in ethanol resulting in a magnetic PUF. A related study synthesized a super-adsorbent PUF coated with iron oxide nanoparticles, and an indolocarbazole based polymer (ICZP6) for the removal of oil and organic solvents (Vintu and Unnikrishnan, 2019). The ICZP6 polymer was synthesized via a coupling reaction between 2, 8-dibromoindolo[3,2-b]carbazole and 9,9-dioctyl-2,7-diethynylfluorene in the presence of trimethylamine, bis(triphenylphosphine)palladium(II)chloride, triphenylphosphine, and copper iodide. This was followed by immersing a PUF into the iron oxide and ICZP6 mixture to yield a coated PUF. Other metal compounds have also been investigated to enhance the properties of PUF. For instance, a polydopamine coated

$AgNO_3$ nanoparticles doped open cell PUF was prepared by immersing PUF in a $AgNO_3$ solution and used in combination with sodium borohydride for the reduction of methylene blue dye (Lefebvre et al., 2017).

4.5. Alginate-PUF composites

Alginate is commonly incorporated into adsorbents because of its high adsorption capacity. Alginate/polyurethane composite foams have been synthesized for selective removal of Pb(II) ions in a polymerization reaction involving a prepolymer derived from toluene diisocyanate and poly(oxy C2–4 alkylene) diol, and sodium alginate in the presence of a tri-block copolymer used as a surfactant (Sone et al., 2009). A similar study synthesized polyurethane/sepiolite cellular nanocomposites for enhanced remediation of nitrates-polluted water (Barroso-Solares et al., 2020). In other studies, alginate-PUF composites were prepared and applied to remove metals in aqueous systems (Sone et al., 2009).

4.6. Graphene-PUF composites

Graphene-PUF composites have been synthesized and applied for the removal of various contaminants in aqueous solutions. Graphene has the advantages of a high surface area and ease of functionalization. For example, a polymer brush graphene-PUF composite was synthesized and applied for selective adsorption and subsequent recovery of precious metal ions from metallurgical slag and aqueous systems (Xue et al., 2019). The NCO groups of an open cell polyurethane were reduced to amino groups under acidic conditions and then added the PUF to a graphene oxide suspension resulting in a graphene oxide coated PU. The sponge was further functionalized coating with polydopamine in an alkaline dopamine solution followed by coating with cysteine methacrylate monomer.

Another study synthesized graphene iron oxide coated PUF by immersing PUF into a pH controlled Fe_3O_4, graphene oxide in water and ascorbic acid dispersion (Anju and Renuka, 2020). A magnetic superhydrophobic PUF loaded with iron oxide, graphene oxide and oleic acid was synthesized and utilized as a high performance adsorbent of oil from water (Khalilifard and Javadian, 2020). A commercial PU was immersed into a graphene oxide oleic acid iron oxide nanoparticles powder dispersion in an alcoholic solution.

4.7. Microbe-impregnated PUFs

The used of microbes in bioremediation of contaminated environmental media has been widely studied. PUF impregnated with microbes have been developed and applied for remediation of contaminants in aqueous systems. Nitrifying sludge immobilized waterborne polyurethane pellets have been synthesized for adsorption of NH_4^+-N from synthetic waste water (Lu et al., 2019). Waterborne PU (10%) and pretreated nitrifying sludge (90%) were reacted in the presence of tetramethylethylenediamine and potassium persulfate to produce polyurethane pellets. In another study, *Rhodococcus* sp. F92 was effectively immobilized on PUF, resulting 10^9 viable cells per cm^3 of PUF (Quek et al., 2006). Other adsorbents based on microbes immobilized on PUFs include: (1) cyanobacterium (*Anabaena* sp. ATCC 33047) immobilized in PUF (Clares et al., 2015), (2) microalgae (*Scenedesmus acutus*, *Chlorella vulgaris*) immobilzed in PUF support (Travieso et al., 1999), (3) seaweed (*Ascophyllum nodosum*) immobilized in polyurethane foam (Alhkawati and Banks, 2004), (4) *Aspergillus terreus* immobilized in PUF (Dias et al., 2002), and (5) a consortium of microorganisms (B350) immobilized in PUF (Zhou et al., 2009).

4.8. Cyclodextrin-PUFs

Cylcodextrins (CDs) are formed via enzymatic reaction of enzymes like 1,4-glucan-glycosyltranferase on starch leading to cyclic oligomers consisting of 6–12 glucose linked by 1,4 linkages (Fallah et al., 2019). The formation of α–, β – and γ– CDs, which contain six, seven and eight glucose units each, respectively, is dependent on the type of transferase enzyme employed along with the reaction conditions. Typically, the secondary OH groups are pointed inwards of the truncated cone while the primary OH groups are pointed outwards of the torus (Morin-Crini and Crini, 2013).

A number of preparation methods for CDs have been reported in literature. For instance, hydroxypropyl-β-cyclodextrin-polyurethane magnetic nanoconjugates/reduced graphene oxide (HPMNPU/GO) supramolecules were prepared by reacting freshly prepared reduced graphene oxide with previously synthesized HPMNPU in deionised water at 50 °C for 5 h (Nasiri and Alizadeh, 2019). Another study synthesized three CD-PUF adsorbents; γ-Cyclodextrin polyurethane polymer (GPP), γ-cyclodextrin/starch polyurethane copolymer (GSP) and starch polyurethane polymer (SPP) to study the mechanism of removal of phthalate esters in aqueous solutions. The adsorbents were separately prepared in a one-step reticulation reaction in dimethylformamide at 70 °C for 1 h using starch, and methylene diisocyanate as cross-linking agents (Okoli et al., 2014). Recently, Leudjo Taka et al. (2020) synthesized a novel biopolymer nanocomposite with inorganic, organic and antimicrobial properties for the removal of trichloroethylene and Congo red dye from wastewater. They reacted phosphorylated carbon nanotubes (pMWCNTs) with hexamethylene diisocyanate as a cross-linker and decorated the resulting polymer (pMWCNT-βCD) with TiO_2 and Ag by a sol-gel method to obtain the biopolymer nanocomposite (Leudjo Taka et al., 2018). Other CDs reported in literature include: (1) epichlorohydrin (EPI) cross-linked β-cyclodextrin polymer (β-CDBEP) for the adsorption behaviors of Eriochrome Black T from water (Li et al., 2019), (2) phosphorylate multiwalled carbon nanotube-cyclodextrin polymer for the removal of cobalt and 4-chlorophenol from synthetic aqueous solutions (Mamba et al., 2013), and (3) silica-based cyclodextrin hybrid porous solids consisting of inorganic silica network with covalently connected cyclodextrin units trapped inside cage-like interconnected micropores for the determination of polychlorinated biphenyls in environmental water (Belenguer-Sapina et al., 2020). However, further research is required to compare the properties and adsorption capacities and selectivity of the CDs to the various PUF adsorbents.

In summary, PUF adsorbents should be systematically prepared under specific classes in order to achieve specific characteristics. These classes should be designed to focus on high efficiency removal of specific types of pollutants, by prioritizing specific surface area, porosity, hydrophobicity, surface functional groups, surface charge, crystallinity and microstructure in varying order and degree. Care should be exercised in the design of PUF adsorbent designated for the removal of general pollutants owing to issues that may arise based on selectivity. Existing studies are silent on the selection criteria of materials to be used as precursors for the development of PUF adsorbents. Here, we propose that the choice of materials should be based on the following: (1) potential to achieve desired physico-chemical properties and contaminant removal performance, (2) ease of regeneration and recycling using low-cost methods, (3) opportunities for biodegradation at the end of the life cycle, and (4) low-cost and ready availability, and (5) low environmental and climatic footprints, including greenhouse gas emissions during production, use, and ultimate disposal. Moreover, the synthesis aspects of PUF-based adsorbent need to take into account the enhanced stability structures in such a way to explore their role in the dynamic adsorption system.

5. Characteristics of polyurethane adsorbents

Following preparation, the properties of the polyurethane adsorbents will need to be evaluated for suitability to remove the targeted pollutants, and this is achieved through a range of techniques. Key characteristics that have a bearing on the adsorptive performance of the materials include hydrophobicity, surface charge, surface functional groups, crystallinity, porosity and specific surface area, and microstructure (de Almeida et al., 2007; Hussein and Abu-Zahra, 2016; Centenaro et al., 2017; Hong et al., 2018; Anju and Renuka, 2020; Barroso-Solares et al., 2020; Eibagi et al., 2020; Guselnikova et al., 2020; Jamsaz and Goharshadi, 2020; Jin et al., 2020; Kalaivani et al., 2016; Amorim et al., 2021). The techniques used are varied, and they include contact angle measurements, zeiter sizer, pH at zero point charge (pHzpc), thermogravimetric analysis (TGA), X-ray diffraction (XRD) spectroscopy, Fourier transform infrared (FTIR) spectroscopy, scanning electron microscopy (SEM), porosimetry, and transmission electron microscopy (TEM). Neutron magnetic resonance spectroscopy has also been used to identify changes in structure following modification (Khan et al., 2015). With the recent advancement in technology, nonintrusive and predictive methods such as modeling, machine learning (mL), artificial intelligence (AI), big data analytics, and artificial neural networks (ANN) are increasingly being used to predict some properties of materials without the requirement of time-consuming and costly synthesis (Li et al., 2020). Neural networks can be used for predicting and processing images such as SEM and TEM images to predict morphological properties like porosity, crystallinity, etc. Despite anecdotal evidence showing there are large volumes of data generated in laboratories, there is limited literature on the use of such techniques on polyurethane adsorbents thus far. The techniques have however, been applied to evaluate related materials (e.g., Paci, 2012; Chen et al., 2019; Yu et al., 2020a, 2020b), and are rapidly gaining research interest. The major challenge though, is that AI and mL requires large volumes of data for training to improve model prediction. Even then, future studies are likely to use these techniques more extensively. For composites, the properties will depend on the individual components such as organic or inorganic materials (Zia et al., 2015). In this section, a few examples of typical characteristics of polyurethane adsorbents are presented, and details are provided in Table 2.

5.1. Hydrophobicity

Hydrophobicity determines the interactions between the polyurethane adsorbent and the pollutant, and is mainly influenced by surface moieties (Zia et al., 2015; Kupeta et al., 2018; Qin and Wang, 2019). Previous research has therefore investigated the hydrophobicity of polyurethane adsorbents. For example, the hydrophobicity of a polyurethane/castor oil biocomposite was attributed to ricinoleic acid, the main constituent of castor oil (Amorim et al., 2021). The linking of the free –N-C=O groups and the OH groups of the residues arises due to the reaction between one of the free isocyanates with castor oil. The motor oil is readily adsorbed with a water contact angle of 0°, showing exceptional superoleoflity. The contact angle is a measure of hydrophobicity, which easily manifests through the wetting properties of the surface. Below 90°, the contact angle indicates favorable wettability, while above 90° wettability is unfavorable. In addition, the biocomposites had an increased contact angle and hydrophobicity, indicating good adherence of the residues to the polymer framework, and subsequently reducing the cavities without the requirement of alkaline treatment (Amorim et al., 2021). In another study, water droplets on the graphene-meso iron oxide-PUF composite formed deformed spherical droplets indicating hydrophobicity (apparent contact angle = 151°) (Anju and Renuka, 2020). In the same study, an oil droplet was immediately absorbed into the adsorbent indicating its oleophilic nature (apparent contact angle = 0°) (Anju and Renuka, 2020). The excellent oleophilic and hydrophobic characteristics of the adsorbent are important for selectively removing oil and organic pollutants from aqueous systems.

5.2. Crystallinity

Crystallinity is a major determinant of the accessibility to internal active sites for both pollutants and water. Previous researches show that a reduction in the crystallinity enhances metal ion sorption, for example (Saranya et al., 2017). Through the use of X-ray diffraction the complexation, crystallization and structure of the polymer matrices can be determined (Saranya et al., 2017). The crystalline phases usually comprise of urethane moieties, the characteristic structural entity in polyurethanes (Li et al., 2020). These are important especially to confirm the incorporation of metal-based components such as Fe_3O_4 into the polyurethane matrix, and can be used to track structural changes due to modification. For instance, PUF has characteristic diffraction peaks around 19°, due to the presence of both hard and soft phases of amorphous polyurethane coupled with its short range well-ordered structure (Anju and Renuka, 2020). In a previous study, the persistence of the peak around 19° demonstrates the polyurethane structure was unaltered by modification (Anju and Renuka, 2020). Further, the disappearance of the graphene oxide peak at 10° indicated the conversion of graphene oxide to graphene. The presence of Fe_3O_4 nanoparticles and the amorphous character of the composite were confirmed by wide angle XRD. Another study used peak ratios to determine the degree of graphitization of polyurethane waste into activated carbon (Li et al., 2020).

5.3. Surface functional groups

The surface functional groups on polyurethane adsorbents play a critical function in adsorption, thereby controlling the adsorption mechanisms. Interactions between the pollutants and the adsorbent surface are largely influenced by the chemistry of the functional groups. For instance, electron-rich moieties such as those containing oxygen or nitrogen atoms have a higher affinity for positively charged pollutants like metal ions or other cationic species. Invariably, characteristic functional groups on the polyurethane structure are: (1) the N-H amine (3330 cm^{-1}, and 1300 cm^{-1}), (2) C-O-C ether groups (1200 cm^{-1}), (3) N-H deformation and C-N elongation vibration of amide II bands (1510 cm^{-1}), and (4) the urethane C=O binding stretch (1650, 1153 cm^{-1}) (Centenaro et al., 2017; Anju and Renuka, 2020; Amorim et al., 2021). In addition to these, the CH_3 and CH_2 deformation on the polyurethane backbone (2926 and 2854 cm^{-1}), and the expected benzene ring vibration (1600 cm^{-1}) are also commonly observed (Centenaro et al., 2017). For composites, a similarity in spectra of the constituent components point to a favorable interface between the polyurethane and the other components. Modification of the polyurethane often results in certain peaks changing in intensity (Anju and Renuka, 2020; Barroso-Solares et al., 2020). For instance, in a previous study the adsorption band at 2300 cm^{-1} showed a reduced intensity, indicating loss of the free NCO moiety. This suggests that the free NCO groups in the PUF structure successfully reacted to produce free cross-linked OH groups, resulting in homogeneity on the interface of the PUF matrix and other components (Amorim et al., 2021). Often, new peaks appear due to additives in the composites. For example, for the Fe_3O_4-modified foam, the Fe-O stretching vibration in Fe_3O_4 (600 cm^{-1}) was detected (Anju and Renuka, 2020), and for sepiolite-modified polyurethane on Mg-OH group (3690 cm^{-1}) was observed (Barroso-Solares et al., 2020). Other studies have used the variations in peak position and intensity to indicate bond cleavage and the formation of new moieties (Kupeta et al., 2018).

5.4. Microstructure and surface morphology

Another important property of adsorbents is the microstructure, which influences the surface morphology and has a bearing on the adsorption process (Anju and Renuka, 2020; Amorim et al., 2021). Images derived from such microscopy techniques as SEM detect open pores on the adsorbent surface, which may confer the large specific surface area to the polyurethane (Kalaivani et al., 2016). Wrinkly and thin layers will improve the surface area without altering the pore sizes so that the adsorbent was suitable for the sorptive removal of oil (Khalilifard and Javadian, 2020). A surface morphology study on a polyurethane/castor

Table 2
The properties and adsorption performance of polyurethane-based adsorbents.

Material	Properties	Pollutant	Regeneration capacity	Reference
PU/castor oil biocomposite	Biocomposite had characteristic FTIR peaks for PU; SEM images show an uneven and continuous macroporous surface with irregular shaped voids of various dimensions and closed and open globular cells; There was insignificant change in the initial degradation temperature of the biocomposite at elevated temperatures; biocomposite was hydrophobic;	Motor oil, 340.7 ± 40.4–827.4 ± 98.1% removal	Removal efficiency of organic solvents and of oil ≤ 82.0 ± 1.7 s and was reusable, retaining hydrophobicity after recycling.	Amorim et al., 2021
PUF decorated with graphene-meso iron oxide composite	The adsorbent had a characteristic XRD peak (19.3°), attributed to short range ordered structure, and soft and hard amorphous phases. The graphene oxide peak (10°) was absent, indicating its conversion to graphene; FTIR spectra showed characteristic NCO peaks (2322 cm^{-1}), C=O stretch (1153 cm-1, 1639 cm^{-1}, and 1734 cm^{-1}), and Fe-O stretching vibration (600 cm^{-1}) due to Fe_3O_4 nanoparticles; TG data indicate the composite was slightly more thermally stable than the pristine PU.	Acetone, bean oil, chloroform, diesel oil, dimethylformamide, dimethylsulfoxide, lubricating oil, tetra hydrofuran, toluene,; Adsorption capacity: 90–316 g/g.	Rapid, selective absorption of oils from aqueous mixture under a magnetic field. The pollutant can be easily recovered after sorption through squeezing without any structural or performance decline. The adsorbent is thus regenerated for more than 150 cycles.	Anju and Renuka, 2020
PU/sepiolite cellular nanocomposites	Modification with a quaternary ammonium salt reduced the nanoparticles specific surface area (398.0–49.1 m^2/g). This indicates that potential enhancement of the removal capacity should be primarily due to chemical affinities. PU with sepiolites content in the range of 1–3% (w/w) showed similar or larger cell sizes, whereas modified sepiolites in the range of 5–8% (w/w) reduced the cell size marginally. Higher sepiolites content (10%) induced agglomeration and breakdown of the cell structure. TGA data confirmed homogeneity of the nanocomposite PU composition, and the final solid residue due to the sepiolite confirmed there was 8 wt% sepiolite in the PU matrix.	NO_3^-, maximum adsorption capacity: 23.30 mg/g.	The adsorbent showed no reduction in nitrate removal capacity after soaking into the PU sponge, and was effectively applied to real water samples.	Barroso-Solares et al., 2020
PUF coated with chitosan film	FTIR data confirmed the characteristics surface functional groups of PU. From the results of the composite, overlap between chitosan and PU peaks was observed.	Reactive blue dye, maximum adsorption capacity of 86.43 mg/g	Even after 7 reuse cycles, the composite efficiently removed reactive blue dye, demonstrating the adsorbent was low-cost.	Centenaro et al., 2017
Unloaded polyether-type PU	–	iron(III)–thiocyanate complexes, q_{max}: 2.06 × 10^{-4} mol/g	Sequential extraction was performed by changing the adsorbent in predefined time intervals, and the results showed about 95% Fe^{3+} removal through 5 successive cycles.	de Almeida et al., 2007
Poly(urethane-imide) containing β-cyclodextrin (β-CD) bound to iron nanoparticles	^{1}HNMR spectra showed the β-cyclodextrin ring protons were high-field (3.11–5.57 ppm). Other peaks were: 7.15–7.95 ppm – aromatic, and 6.99 and 9.13 ppm – amide N–H moieties. The XRD spectrum for the modified PU showed patterns associated with Fe_3O_4 the polymer structure. The β-CD monomer lost its crystallinity by being grafted to a polymer and covers the PU structure without aggregating. The composite decomposed in the temperature range of 30–700 °C in five steps. The globular geometry of dispersed Fe nanoparticles in the PU matrix appeared in the SEM image. Increased intensity of O peak, and emergence of Fe peak in the EDX pattern for modified PU relative to the spectrum for β-CDPU, confirm the effective introduction of magnetic	*Staphylococcus aureus* and *Escherichia coli*, Removal efficiency: 87.39–97.56%	The adsorption capacity of the foam was increased through binding it to magnetic nanoparticles, and it readily separated from the aqueous solution by a magnet.	Eibagi et al., 2020

(*continued on next page*)

Table 2 (*continued*)

Material	Properties	Pollutant	Regeneration capacity	Reference
	nanoparticles to the surface of the modified PU.			
Magnetic PU modified with 3,5-bis(trifluoro-methyl)benzenediazo-nium tosylate	Pristine PU showed characteristic FTIR peaks, a water contact angle of 101 ± 1° and surface free energy of 72.5 ± 0.8 mN/m. This is typical PUs. Following modification, more FTIR peaks emerged (1280 and 1177 cm^{-1}), attributed to the main vibrational modes and rocking vibrations of the modifying agent. Water contact angle increased to 148 ± 1° along with a reduction in surface free energy (72.5 ± 0.8–38.4 ± 0.6 mN/m), suggesting the introduction of low surface energy moiety in the PU structure. The XPS spectrum of pristine PU showed characteristic peaks (288–284 eV, C 1 s, 531.5 eV, O 1 s, and 398.5, N 1 s), whereas subsequent to modification a F 1 s peak (689 eV) and peaks ascribed to the modifying agent, CN/CO, and CH/CC bonds (292.7, 286.5, and 284.5 eV) emerged. Moreover, the CC/CH peak intensity showed an increase. The findings suggested the PU was effectively grafted by 3,5-bis(trifluoromethyl)benzenedia-zonium tosylate. After incorporating Fe nanoparticles into the functionalized PU, Fe-related peak (706–732 eV) and a significant increase in the content of F (2.97–11.63%) was observed.	Organic solvents, oils (rapeseed and pump); adsorption capacity: 40–75% w/w	The adsorbent had magnetic and superhydrophobic characteristics suitable for separating oil/water, and simple recovery by using an external magnetic field.	Guselnikova et al., 2020
Carboxymethylated cellulose nanofibrils embedded in PUF	Unmodified PU showed a smooth continuous surface, whereas the composite foams had a rough surface on increasing the nanofibril content. Pore sizes reduced significantly pristine PU to the composite, while porosity does remained unchanged. The surface area for the composite increased 1.5 fold relative to pristine PU. Pristine PU had a low tensile strength (0.16 MPa) due to the amorphous character of the adsorbent. Addition of the composite significantly enhances the tensile strength. Typical PU FTIR peaks were observed. The carbonyl hydrogen-bond index decreased with increasing nanofibril content.	Cu^{2+}, Cd^{2+}, Pb^{2+}, q_{max}: 78.7, 98, and 216.1 mg/g	Using dilute HCl for desorption, nearly all the adsorbed ions desorbed. The regenerated adsorbent retained 49%, 34%, and 75% removal efficiency. Despite requiring additional fortification, the regeneration efficiency indicates the possibility of recycling the adsorbent is promising.	Hong et al., 2018
Iron oxide nanoparticles incorporated into a porous PUF	The SEM images for the composite show distinctive differences in the cellular structures of the two components. A disorderly cell distribution was observed. The structure confers a larger surface area with iron oxide nanoparticles instead of placing them on the foam surface only.	Arsenic, 40% removal through single stage batch experiments. A multi-stage system can significantly improve removal.	–	Hussein and Abu-Zahra, 2016
Seashell-modified PU sponge	The XRD spectrum for the adsorbent showed characteristic peaks in addition to the peak at ~36.12° due to the $Ca(OH)_2$ (101) crystalline plane. The FTIR spectrum for seashells exhibits peaks due to C–O stretching. The O-H stretching band was at ~3482 cm^{-1}. Following calcination, the band intensities were reduced due to the partial conversion of $CaCO_3$ to CaO. The water contact angle for the adsorbent increased from 94.01 ± 1.23° to 161.06 ± 1.70° after coating it with calcined shells. The high hydrophobicity of the shells emanates from its rough surface. Pristine PU had an interconnected 3-dimensional porous structure, making it appropriate	Organic solvents (ethyl acetate, ethanol, acetone, 2-propanol) Oil (olive oil, crude oil, sesame oil, hydraulic oil, cooked oil); 28.03–42.17 g/g	q_{max} unchanged after 10 reuse cycles. The removal efficiency of the adsorbent was in the range of 28.03–42.17 g/g. There were no secondary pollutants in the oils subsequent to each regeneration cycle, suggesting structural stability of the adsorbent.	Jamsaz and Goharshadi, 2020

(continued on next page)

Table 2 (*continued*)

Material	Properties	Pollutant	Regeneration capacity	Reference
	for the removal and storage of oil. SEM image of pristine PU exhibits a smooth unwrinkled surface, and this smoothened following surface modification.			
PUF based on dopamine derivative	The adsorbent surface was even. Following adhesion with dopamine derivative, the surface developed roughness relative to pristine adsorbent, and the number of nanoparticles adhering onto the surface increased, creating more reactive sites for further functionalization. The zeta potentials of the adsorbents were in the range of − 11.2, to − 39.1 mV, showing the foam became increasingly negative; Characteristic FTIR peaks were observed.	Methylene blue, 98.9% removal.	When the adsorbent was reused for 10 cycles, the removal efficiency decreased to 41.8%, showing the adsorption capacity had nearly reached saturation point.	Jin et al., 2020
Hyperbranched PU resins	FTIR and ^{1}HNMR spectra were characteristics for PU-derived adsorbents. The PUF exhibited the NCO amide (II) peak (1497 cm^{-1}). The adsorbent was stable ≤ 220 °C, therefore it is useful for high temperature applications. The adsorbent has a porous surface where metal pollutants can be adsorbed. EDX data exhibit only C, N, O peaks which make up the polymer framework. Besides C, N, O peaks, the EDX spectrum for Ni^{2+} loaded adsorbent had S and Ni peaks signifying Ni^{2+} adsorption.	Pb^{2+} and Ni^{2+}, 236.5 and 217.5 mg/g	5 reuse cycles were performed, and rate of desorption was rapid, (highest desorption within 1 h), for Pb^{2+} and Ni^{2+}. The reuse experiments show that adsorption by the PU is reversible.	Kalaivani et al., 2016
PUF decorated with Fe_3O_4@oleic acid@graphene oxide	The modified foam was hydrophobic (contact angle =158°). The PU adsorbent selectively removed organics and oils from aqueous solution with high adsorption capacity. The adsorbent had a porous 3-dimensional microstructure with an even surface and pore size 200–600 µm. Upon deposition of the Fe_3O_4-based nano-sheets onto the PU framework, the even surface was covered by a thin wrinkled sheath of nano-sheets. This created a wrinkled and rough surface, generating an entirely different surface morphology. EDX analysis and elemental mapping showed the constituent elements on the nanosheets (i.e. C, O and Fe) were evenly dispersed in the 3D structure of the foam. Owing to the low nanosheet content, the difference in the thermal stabilities of the materials is insignificant. Introducing oleic acid did not make a practical impact on the crystalline structure of the Fe nanoparticles.	Chloroform, toluene, olive oil, canola oil, acetone, kerosene, Yadavaran, THF, Dehloran, hexane, DMSO, removal capacity was in the range of 40–120 g./g.	Fe_3O_4 nanoparticles were utilized because of low cost, large specific surface area, magnetization capabilities, and ecofriendliness. The modified foam can be easily removed by a magnet after exhaustion to 15 cycles.	Khalilifard and Javadian, 2020
Multi-walled carbon nanotube–PU composite	FTIR identified characteristic PU groups. The specific surface area of the adsorbent (491 m^2/g) was greater than pristine multi-walled carbon nanotubes (158–162.16 m^2/g. The pore radius (1.11–1.61 nm) showed mesoporosity. SEM images showed an irregular, porous structure.	Safranin T, Pb^{2+}, *Batch experiments* q_{max}: 500 mg/g (Safranin T) and 270.27 mg/g (Pb^{2+}). *Column studies:* breakthrough = 425.25 mg/g (Safranin T) and 239.05 mg/g (Pb^{2+}).	Adsorption efficiency reduced from 96% to 73% (Safranin T), and from 95% to 68% (Pb^{2+}) after the 4th cycle. The 27–32% reduction was attributed to the adsorbent loss during regeneration processes.	Khan et al., 2015
Coal-modified PUF	FTIR data was typical, but the isocyanate peak (2270 cm^{-1}) is absent, implying the reaction went to completion. Modified adsorbents possess voids. Pore density increased with the incorporation of coal. Thermal stability of the composite adsorbent was considerably enhanced.	Brilliant green, 134.95 mg/g	Adsorption efficiency maintained at 93.30%, and did not decline after 4 reuse cycles.	Kong et al., 2016
Cellulose nano-whiskers-based PUF	The nonappearance of NCO stretching (2270 cm^{-1}) from FTIR spectra confirmed the depletion of MDI in	Methylene blue, 554.8 mg/g	Maximum retention capacity of 554.8 mg/g was achieved after 15 reuse cycles.	Kumari et al., 2016

(*continued on next page*)

Table 2 (*continued*)

Material	Properties	Pollutant	Regeneration capacity	Reference
	forming the adsorbent. The XRD pattern for the composite was sharper than for pristine cellulose, indicating a more refined crystalline structure of the composite than cellulose. Average particle size: 197.3 nm. TEM images for the composite showed porosity, which is facilitates accessibility of pollutant to the PU adsorbent.			
PU cross-linked pine cones	FTIR showed characteristic PU linkage peaks; TGA data show that Fenton processing decreased the thermal stability of the pine cone. Fenton pre-treatment enhanced crystallinity and this is attributable to decomposition and removal of resin acids and waxes therefore increasing the lignocellulose content. On cross-linking, the small pores on Fenton pre-treated pine was disappeared, presumably covered by the PU molecules. Specific surface area, pore sizes, and pore volume were thus reduced. The adsorption process is thus likely to be governed by surface phenomena.	2-nitrophenol, pristine, Fenton pre-treated and Fenton pre-treated cross-linked samples: 41.17, 65.75 and 78.05 mg/g.	Adsorption capacity reduced with more reuse cycles. The decrease was lower for pristine (27.27–21.65 mg/g), Fenton pre-treated (46.35–39.02 mg/g) and Fenton pre-treated cross-linked (51.65–41.29 mg/g).	Kupeta et al., 2018
Polydopamine PU open cell foam	SEM images showed good deposition of charcoal microparticles and agglomerated carbon nanotubes	Methylene blue, 245 mg/g removal	Following desorption, the adsorbent could absorb methylene blue to the same extent as runs 5 and 6.	Lefebvre et al., 2018
Polydopamine-coated open cell PUF	SEM imaging showed a rough surface with dispersed aggregates.	Methylene blue, Used as a catalyst support. 30.2 mg/g	The adsorbent can be regenerated efficiently through exposure to air at room temperature for a number of days. The regenerated adsorbent had > 81% methylene blue removal after 25 min (compared to 91% removal in the first run), and then declined gradually in the subsequent runs.	
Activated carbon synthesized using PU waste	H/C ratio: 1.37 - rationalized by detecting alkane groups. Specific surface area: 221–1034 m^2/g;	Malachite green, 428 mg/g removal.	–	Li et al., 2020
Waterborne PU pellets	The pellets had highly porous fibrous structures, which confers them with a high adsorption capacity.	NH_4+-N, 0.0446–0.0504 mg/g removal	–	(Lu et al., 2019)
Sulphonated PU cubes	FTIR spectra were typical for PU, and had additional sulfate groups; Chemical stability of the adsorbent was studied following sequential acid/alkali treatment. This treatment did not significantly affect adsorption as shown by lack of irregularities in pores on SEM images.	Ni^{2+}, 24.39 mg/g removal.	Regeneration was studied by loading Ni^{2+} solution on the adsorbent and eluting with dilute HCl. The adsorption capacity was unaltered for 5 successive cycles, and there was a decrease in Ni^{2+} uptake in further runs.	Mangaleshwaran et al., 2015
Algae-based PU film	FTIR spectra typical for PU. The characteristic peaks for algal cellulose are observable in the spectra for the composite, ascribed to C–H or C–O or C–C bonds. Amide I and amide II bands imply the presence of protein groups, common in biomaterial. SEM images show salt crystals, possibly due to algae source. On the film, the smooth sheet is wrapped around the outer layer, and the supporting layer is visible on the cross-section. The film resembles membrane structure, signifying potential application in membrane filtration processes. The adsorbent contained the thermally stable urethane linkage.	NH_3–N, 187.84–393.43 μg/g	–	Marlina et al., 2020
PU-palm fiber biocomposites	The pore size was reduced relative to the pristine PU following introduction of fibers to the polymeric structure. The biocomposites possessed irregularly shaped open interconnected pores of various sizes, with an uneven continuous surface. With an increase in fiber content, there was a corresponding	Diesel S-10 oil, 10.02 g/g)	Oil sorption reduced between 5 regeneration and reuse cycles. In the initial cycle, the sorption capacity decreased to 0.70 g/g, at 8.38% efficiency.	Martins et al., 2020

(*continued on next page*)

Table 2 (*continued*)

Material	Properties	Pollutant	Regeneration capacity	Reference
	rise in specific surface area ≤ 118.6%. The adsorbents are hydrophobic with a water contact angle > 90°. Introduction of fibers resulted in structural changes in comparison to pristine PU, showing a broad peak (~19°) related to cellulosic material with semi-crystalline domains. The peak around 19 is ascribed to chemical interactions between the PU and the fiber. The FTIR patterns for pristine PU and the composites had some similar features, indicating a favorable fiber/matrix interface. A band intensity reduction at 2273 cm^{-1} was ascribed to NCO.			
p-tert-butyl thiacalix[4] arene imbedded flexible PUF	Introducing thiacalix[4]arene tetrasulfonate in the PU structure resulted in a reduction in water absorbency relative to the pristine material. This can be attributed to hydrophobicity of thiacalix[4]arene tetrasulfonate macrocycles. The foam possessed roughly open cells with a skewed cell size distribution. It is also supposed that uneven cell structure in the composite is primarily caused by high viscosity resulting from the incorporation of thiacalix[4]arene tetrasulfonate into the foam matrix. The increase in T_{onset}, $T_{5\%}$, $T_{10\%}$, $T_{50\%}$ and T_{max} for the composite adsorbent can be ascribed to the high thermal stability of TC4A arising from its aromatic groups which postpone the degradation of the PU adsorbent.	Malachite green, 58.82 mg/g	–	Mohammadi et al., 2014
Sulfonated thiacalix[4] arene-sodium alginate-based PU membrane	Vibration peaks due to alginate carboxylate moieties and the OH peak (~3350 cm^{-1}) confirmed the introduction of sodium alginate inside the foam matrix. The XRD spectrum shows a wide and low-intensity peak (~2θ=24.1°), indicating the roughly amorphous surface. The temperatures at which maximum thermal degradation occurs for the composite rises with tetrasulfonate-sodium alginate content. SEM images show significant porosity relative to pristine material. This is caused by high phase separation in the morphology of soft and hard domains, localizing mechanical stress at the broad regions of hard domains on application of a strain. The hydrophilicity of the composite is higher than that of pristine materials.	Desalination of water through reverse osmosis.	–	Mojerlou et al., 2019
PUF	The pHzpc was 7.26, meaning for pH< 7.26, the adsorbent surface carries positive charge, whereas for pH> 7.26, the surface carries a negative charge. FTIR spectra are characteristic for PU.	Direct Red 80 and Reactive Blue 21, 4.50 and 8.31 mg/g removal	–	Neta et al., 2011
PUF modified with nanoclay	FTIR spectra are characteristic for PU. The 2% (w/w) cloisite 20 A nanocomposite had no XRD peak owing to exfoliation in which layers are entirely dispersed in the PU matrix. The 3 wt% nanocomposite showed a shifted peak with reduced intensity due to intercalation. The 4% (w/w) cloisite 20 A nanocomposite the peak is occurred around 1.7°, revealing intercalation of the nanoparticles. SEM images show a change in pore geometry after introducing nanoclay to the PU matrix. Pore radius reduced and the pore volume is more homogeneous.	Oil, ≤ 56% removal	Chemical recovery resulted in increased adsorption capacity.	Nikkhah et al., 2015
		Pb^{2+}, q_{max}: 169.52 mg/g	–	

(*continued on next page*)

Table 2 (*continued*)

Material	Properties	Pollutant	Regeneration capacity	Reference
Nanochitosan /PU /Polypropylene glycol ternary blends	Frequency shifts and the emergence of a new peak confirms effective blending. This proves the ternary blend with Gluteraldehyde ratio was more thermally stable relative to the blend without Gluteraldehyde. This was confirmed by the higher T_g. The adsorbent had numerous cavities and enhanced porosity. From SEM imagery, the components were well mixed. The adsorbent surface was rough compared to the pristine material.			Saranya et al., 2017
Self-assembled 3D Mg $(OH)_2$ coated granular PU	The adsorbent structure with particle sizes in the range of 210–841 mm is concave/hollow, showing a smooth nonporous surface. Following incorporation of MgOH, the sharp FTIR peak (1512 cm^{-1}) was reduced, implying the N on the composite might be removed during hydrothermal treatment. BET surface area was 20.2 m^2/g, which is higher than the individual components.	Cu(II), Cd(II), and Pb(II), 472, 1050, and 1293 mg/g adsorption capacity	–	Vafaeifard et al., 2019
PUF membrane modified with humic acid-chitosan cross-linked gels	Highly porous and flexible, with a porous hollow knitted net structure; XPS data for the composite showed a new peak emerging, suggesting the surface of chitosan was successfully decorated with humic acid. The major decomposition temperature of the composite was 6 °C less than that for raw chitosan.	Methylene blue, rhodamine B, methyl orange; 62.1%, 71.6%, 97.7% removal	The retention efficiency for methyl orange and rhodamine B declined gradually with increasing number of regeneration cycles. After the 4th cycle, retention efficiency was 90.4% (methyl orange) and 94.0% (Rhodamine B) of its initial cycle use.	Yang et al., 2017
Graphene–PU composite	Microstructure images showed a cracked structure formed by bond cleavage, and the surface was stripped upon hydrolysis, increasing hydrophilicity and created a suitable interface with graphene oxide. The composite superstructure showed a rough surface due to graphene layers. FTIR data showed that functionalization was successful.	Au^{3+}, Pd^{2+}, Pt^{4+}, and Ru^{3+}, q_{max}: 1111.1, 819.7, 584.8, 290.7 mg/g	The removal of the ions reduced by about 5% the initial efficiency after 5 reuse cycles, implying the potential of the adsorbent to selectively remove metal ions.	Xue et al., 2019

oil biocomposite for the adsorption of motor oil showed macroporous foams with an uneven surface, characterized by different sized pores of irregular geometry containing closed and open globular cells, which potentially affect the sorption capacity (Amorim et al., 2021). Further, an increase in the waste content reduced the size of the cavities, increased the pore density, and created more heterogeneous and malformed cellular structures with the capacity to adsorb guest molecules (Amorim et al., 2021). In most cases, polyurethane adsorbents have an intrinsic porous structure and surface heterogeneity. Sorption of pollutants occurs in the cavities of these porous structures. Moreover, structural roughness influences wettability (Anju and Renuka, 2020). Overall, modifying polyurethanes with nanomaterials produced higher surface areas resulting from an inhomogeneous surface, which is usually uneven and wrinkly.

5.5. *Thermal stability*

Thermal properties of an adsorbent are important especially when the adsorbent has to be used at elevated temperatures. The glass transition temperature (T_g) provides information on the thermal stability of the polyurethane adsorbent, where a higher (T_g) indicates greater thermal stability (Saranya et al., 2017). The thermal decomposition pattern is determined using thermogravimetric methods and derivative curves, which illustrate the stages involved. For instance, the degradation curves for a polyurethane/castor oil biocomposite showed two stages: (1) degradation, and (2) subsequent loss of weight caused by the cleavage of the urethane bonds (Amorim et al., 2021). The mechanisms for the disruption or cleavage of the urethane groups involve: (1) dissociation of NCO and OH groups, (2) olefin and primary amine formation, and (3) secondary amine formation. The second stage has been attributed to the breaking of the polyol ester bond. Based on this data, the polyurethane/castor oil biocomposites are usable within a temperature range not exceeding 284 °C. Another study on polyurethane-Fe_3O_4 composites observed a considerable weight loss at temperatures ranging from 200 to 350 °C, which was attributed to the combustion of the carbon backbone (Anju and Renuka, 2020). Generally, composites have a higher thermal stability than pristine polyurethanes, and are thus usable at higher temperatures.

5.6. *Porosity and BET surface area*

The textural properties of polyurethanes are critical for providing information on porosity and specific surface area, and consequently adsorptive performance of the adsorbents. Therefore, these have been measured in several previous studies. For instance, treatment of polyurethane/sepiolite cellular nanocomposites with quaternary ammonium salts for the removal of NO_3^- reduced the specific surface area by about 88% (Barroso-Solares et al., 2020). Other studies have reported an increase in the porosity and surface area following modification (Zhuang et al., 2016; Nethaji et al., 2018; Xue et al., 2019). The increased surface area results in a corresponding increase in active adsorption sites, and consequently the adsorption capacity (Xue et al., 2019).

5.7. Other properties

In addition to the foregoing commonly used parameters, polyurethane adsorbents have also been characterized to determine the elemental composition. This is usually achieved using; (1) energy dispersive X-ray (EDX) spectroscopy coupled to SEM, or (2) separately as using x-ray photoelectron spectroscopy. Data on the elemental composition of PUF adsorbents provide insights into the success and nature of modification. Surface charge can also be determine using zeta potential or pHzpc as proxies (Kupeta et al., 2018). The pHzpc determines the pH at which the surface of the adsorbent is uncharged (Neta et al., 2011). Mechanical strength has also been used to evaluate polyurethane polymers, where good mechanical strength is important in practical applications such as in oil adsorption at elevated temperatures (Jamsz and Goharshadi, 2020). Moreover, good mechanical characteristics are particularly important in films and membranes, where the adsorbent material needs to be mechanically strong to withstand water pressure (Marlina et al., 2020). Magnetic behavior is important, especially for recovering the spent adsorbent using an external magnet (Khalilifard and Javadian, 2020).

In summary, depending on the precursor material and preparation methods, the PUF adsorbents varied considerably with respect to surface area, crystallinity, functional groups, thermal stability, hydrophobicity, and pore structure (Table 2). In turn, these properties include the contaminant removal capacity, and suitability of the adsorbents for various remediation applications. Specifically, PUF adsorbents are suitable for the removal of contaminants in aqueous systems owing to: (1) a well-developed porous structure which confers it with a high surface area, (2) hydrophobicity, which is suitable for selectively removing organic pollutants, (3) electron-rich surface functional groups, which can be useful in targeting toxic metal pollutants, (4) crystallinity, which determines the accessibility to internal active sites for pollutants and water, and (5) thermal stability, which permits usage at high temperature applications. A key strength of PUF is its ease of modification to tailor the properties for targeted adsorption applications. Moreover, because spent adsorbents can easily be regenerated for multiple reuse, this significantly reduces the cost associated with the PUF adsorbents.

5.8. Regeneration, reuse, and recycling

The capacity of adsorbents to be recycled for multiple reuse is crucial for lowering costs. In the case of PUF adsorbents, their capacity to be regenerated using simple and inexpensive means, and through a number of cycles, is its major strength. This significantly reduces the environmental footprint, and also makes it attractive for use in large scale applications. Consequently, to demonstrate cost-effectiveness, most researchers have regenerated and reused the adsorbents. The regeneration methods range from mechanical compression to chemical treatments. Using mechanical compression, a previous study evaluated the pollutant release and reuse of polyurethane/castor oil biocomposites over 10 cycles by manual compression and solvent release (Amorim et al., 2021). The results showed that diesel residues caused a decline in hydrophobicity of up to 38.1 for the composites. Using the solvent release method, hydrophobicity decreased by up to 7.5. Another study demonstrated that, due to the inherent elasticity of the graphene-meso iron oxide composite incorporated into the PUF, the adsorbent can be reused over 150 cycles by manually squeezing out the pollutant without any decline in the structure and performance (Anju and Renuka, 2020). Yet another study showed that, chitosan-coated polyurethane was efficient in removing reactive blue dye even after seven regeneration cycles (Centenaro et al., 2017). Although reusable over a large number of cycles relative to other adsorbents, the adsorptive performance of PUF decreases with time. Overall, mechanical regeneration of the polyurethane adsorbents by compression takes advantage of the elasticity of the foam, while chemical treatments use the ion exchange or other properties that can be chemically reversed.

6. Application of polyurethane-based adsorbents

Pristine polyurethanes have been investigated for the removal of various pollutants. However, compared with modified polyurethanes, the removal capacities are lower. For instance, an acerola residue-modified polyurethane-castor oil composite (adsorption capacity for oil: 827.4 ± 98.1%) was a more effective adsorbent than the pristine equivalent (Amorim et al., 2021). Another study showed that the adsorption capacity of polyurethane foam modified with graphene-meso iron oxide (90 g/g to 316 g/g) was higher than that of graphene coated polyurethane sponges (80–180 g/g) (Anju and Renuka, 2020). As a result, numerous studies have focused on removing pollutants using polyurethanes with various modifications such as composites with vegetable oils (Amorim et al., 2021) magnetic nanoparticles (Hussein and Abu-Zahra, 2016; Guselnikova et al., 2020), graphene composites (Anju and Renuka, 2020), sepiolite cellular nanocomposites (Barroso-Solares et al., 2020; Yu et al., 2020a,2020b), polyurethane foam decorated with chitosan (Centenaro et al., 2017), starch-modified foam (Zia et al., 2015), MgOH-coated (Vafaeifard et al., 2019) and poly (urethane-imide) containing β-cyclodextrin bounded to iron nanoparticles (Eibagi et al., 2020). Detailed presentations of various categories of polyurethane-based adsorbents are given in previous reviews (Zia et al., 2015; Taka et al., 2017) and in Tables 1–4.

6.1. Metals, metalloids, and rare earth elements

PUF adsorbents have been used for the removal of metals (e.g., Cd, Zn, Cr, Cu, Fe, Ca, Ni, Co, Mg, Mn, Pb), metalloids (Bi, Sb), and rare earth elements (e.g., dysprosium) in aqueous systems. Table 3 summarizes the nature of the PUF-based adsorbents, contaminants investigated, and key results, including removal mechanisms such as adsorption kinetics, thermodynamics, and isotherm models. For example, cyanobacteria (*Anabaena* app) immobilized on PUF removed 162 mg/g of Cd(II) equivalent to 80% off the initial concentration (Clares et al., 2015). The same study reported fast adsorption which followed a Langmuir isotherm model. (Micro)organisms (e.g., bacteria, fungi, seaweed) immobilized on PUF, and alginate-PUF composites were also used for the removal of metals (Cu, Ni, Fe) (Dias et al., 2002; Alhakawati and Banks, 2004; Sone et al., 2009).

Rhodamine B grafted PUF removed 670–80% of Bi(III), Fe(III), and Sb(III) in aqueous solutions in both column and batch experiments. Results showed that adsorption followed first order kinetics and fitted the Morris-Weber model for particle diffusion. The average Gibbs free energy (−6.6 kJ/mol) indicated spontaneous chemisorption. Optimum pH for adsorption was less than 1–3, and the selectivity sequence in the pH range 1–3 followed the decreasing order: Fe(III) followed by Sb(III) then Bi(III). This trend reflected the differences in ionic sizes of the species. The same study also investigated the role of ligand concentration (i.e., thiocyanate), and observed that optimum concentration for the maximum adsorption were: 0.65–5 mol/L for Bi(III), 1.3–5 mol/L for Fe(III), and 2.5–5 mol/L for Sb(III). In the column experiment, saturation occurred after passage of 110–160 mL and the breakthrough values (mmol/g) for column experiments were: 0.03 for Bi(III), 0.06 for Sb(III), and0.08 for Fe (III).

Using PUF-supported graphene oxide–titanium phosphate, a high maximum adsorption capacity (576.17 mg/g) of the rare earth element (dysprosium) was observed (Peng et al., 2021). In the same study, the adsorption of dysprosium on PUF adsorbents followed the pseudo-second order kinetic and the Langmuir isotherm models (Peng et al., 2021). The removal occurred over a wide range of salinity and pH conditions via electrostatic interactions. However, the bulk of the studies considered single element systems, while those investigating complex systems (ternary, quaternary) with potential interactions are still limited.

Table 3
Removal of metals, metalloids, and rare earth elements by polyurethane-based adsorbents.

Adsorbent	Contaminants	Experimental conditions	Results	References.
Trace metals:				
Cyanobacterium (Anabaena sp.) immobilized in PUF	Cd (II)	Batch experiment using 100 mg/L synthetic CdCl2 solution.	Fast removal of 80% in 10 min\ Adsorption capacity (q_{max}): 162 mg Cd(II)/g of dry biomass equivalent to 80%Data fitted Langmuir model	Clares et al., 2015
Microalgae (Scenedesmus acutus, Chlorella vulgaris) immobilzed in PU support	Cd, Zn, Cr	Packed bed column with microalgae in PUF. Synthetic solution of various concentrations of metals tested.	Maximum removal: 57% Cd, 78% Zn, and 34% Cr. Microalgae species were tolerant to typical concentrations of metals in wastewaters	Travieso et al., 1999
Seaweed (*Ascophyllum nodosum*) immobilized in PUF	Cu(II)	Batch experiment compared immobilized versus free seaweed using synthetic solution of 0.0315 mmol/dm^3 Cu(II) at 293 K: agitation: 200 rpm; pH: 5, 5 and 7; Adsorption/desorption experiments were conducted at 0.0315 and 0.944 mmol/dm^3 at pH 5 after 5 cycles	Adsorption capacity: 0.037 mol Cu(II)/g Removal: 85% Regenerated adsorbent had low adsorption stabilizing at 0.23 mmol/g after 3 cycles. pH effect: q_{max} increased from 0.55 and 0.416 mmol Cu/g for immobilized biomass when pH was reduced from 4.0 to 3.0, Temperature effect: q_{max} improved from 0.576 mmol /g (283 K) to 0.636 mmol/g (303 K).	Alhakawati and Banks, 2004
Aspergillus terreus immobilized in PU	Cr, Ni, Fe	Batch experiments using three metallurgical effluents for a steel foundry conducted at agitation, 200 rpm, temp: 28 ± 3 °C, and initial pH: 4.5 Concentrations: Effluent 1: 65, 4.9, and 25 mg/L for Fe, Cr, and Ni, respectively. Effluent 2: 46, 4.7, and 21.2 mg/L for Fe, Cr, and Ni, respectively. Effluent 3: 730, 157, and 60 mg/L for Fe, Cr, and Ni, respectively. Effluent had a pH 1.0 and were diluted prior to adsorption experiments	Maximum metal uptake in a medium with 100% effluent and 1% glucose after 6 days were: 164.5, 96.5, and 19.6 mg/g for Fe, Cr, and Ni, respectively. Metal uptake varied strongly: 43.8–244á. mg/g Fe, 1.9–26.6 mg/g Ni, and 8.6–96.5 mg/g) Cr. Metal removal decreased as concentration increased, and as Fe/Cr ratio exceed 1.0.	Dias et al., 2002
Alginate/PU composite foams	Ca, Cd, Co, Mg, Mn, Pb	Agitated batch experiments testing composite and sole PU using a multi-element synthetic metal solutions at pH 0.98, 2.05, 3.02, and 3.96. Details of concentrations, and agitation speed used not provided.	Adsorption followed Langmuir model with adsorption capacity (mol/g) of: 17.06 Ca, 14.66 Cd, 15.53 Co, 8.84 Mg, 16.18 Mn, and 15.95 Pb.Highly acidic pH (0.98, 2.05) reduced adsorption. Pb(II) adsorption on composite reached equilibrium within 15 min, but sole PU showed very little capacity to remove Pb(II). Competing ions reduced selectivity and adsorption capacity of Pb, but effect was less than that of pH. Composite was very stable, flexible, simple to use, and reusable following regeneration with ethylenediamine-N,N,N,N-tetraacetic acid) disodium salt.	Sone et al., 2009
PUF onto which was grafted Rhodamine B	Bi^{3+}, Sb^{3+}, Fe^{3+}	Both batch and column experiments using synthetic solutions. Batch experiment at 25 °C and 2 ug/mL, at contact time 1–60 min and variable pH (<1–6) and ligand (thiocyanate) concentration. Packed bed column experiment with flow rate of 3 mL/min	Adsorption kinetics were fast with 70–80% adsorbed within 5–10 min). Adsorption followed first order kinetics and fitted the Morris-Weber model for particle diffusion. The average Gibbs free energy: 6.6 kJ/mol indicating spontaneous chemisorption. Optimum pH for adsorption was less than 1–3, and the selectivity sequence in the pH range 1–3 reflected difference in ionic size and was in the order: Fe^{3+}>Sb^{3+}>Bi^{3+}. Optimal thiocyanate concentration for q_{max} were: 0.65–5 for Bi^{3+}, 1.3–5 for Fe^{3+}, and 2.5–5 for Sb^{3+} mol/L. Saturation occurred after passage of 110–160 mL and the breakthrough values (mmol/g) for column experiments were: 0.03 for Bi^{3+}, 0.06 for Sb^{3+}, and 0.08 for Fe^{3+} mmol/g.	
PUF-supported graphene oxide–titanium phosphate	Rare earth element (dysprosium)	Batch experiments to determine adsorption capacity.	Excellent adsorption capacity: 576.17 mg/g. Data obeyed Langmuir model and pseudo-second order kinetics with half-equilibrium achieved within 2.5 min Adsorption occurred at a wide range of pH and salinity. Strong phosphate binding to Dy^{3+}, improved removal via electrostatic interaction.	Peng et al., 2021
Microorganisms (B350) immobilized in PU (IPU) foam and sole PU	Cu(II)	Batch experiments compared sole PU and that with immobilized B350 (IPU) using synthetic solution: Agitation: 150 rpm Contact times: 5, 10, 20, 30, 40, 60, 90, 120,150, 240, 300, 480 and 720 min Concentrations: 20, 40, 60 and 80 mg/L pH: 2–8 Temperature: 15, 22, 28, 30, 36, and 40 °C.	Data followed pseudo-second-order rate model, and Langmuir isotherm. Removal of IPU was about double that of PU for all operating conditions. Maximum adsorption occurred at pH 6 but decreased with pH due to competition with protons. Temperature had a minor effect although a general increase in adsorption with temperature was observed. Saturation occurred within 240 min, and IPU showed a faster removal rate than PU.	Zhou et al., 2009

6.2. Dyes

The application of PUF-based adsorbents for removal of dyes including those used in textile and food industry has received significant research attention (Table 4). The PUF adsorbents reported in literature include lignin-PUF, and chitosan-PUF composites, polyester-based PUF, and sole PUF (Neta et al., 2011; Kumari et al., 2016; Tikhomirova et al., 2018). Results from batch experiments showed that chitosan-PUF composite had an adsorption capacity of 30 mg/g for Acid violet 48. The adsorption of Acid violet 48 followed the pseudo-second order kinetic model, and Langmuir isotherm model for monolayer adsorption. Kumari et al. (2016) investigated the comparative adsorption of cationic (Malachite green) and anionic (Methyl orange) dyes on lignin-polyurethane (LPUF) composite adsorbent. The results showed

Table 4
Removal of various organic contaminants in aqueous systems by polyurethane-based adsorbents.

Adsorbent	Contaminants	Experimental conditions	Results	References.
Dyes:				
Chitosan/PU composite	Acid violet 48	Batch experiment at pH 7 and temperature 30 °C	Adsorption capacity: 30 mg/g Data obeyed pseudo-second order kinetic and Langmuir isotherm models	
Commercial ether-based PUF	Five synthetic anionic food dyes (3 sulfoazo dyes; a quinophthalone dye; and a triphenylmethane)	Batch experiment to investigate pH (<1 −010), contact time (15, 30, 60, 180 min), and ionic strength (0–1 mol/L NaCl at 0.1 mg/L. Data on agitation not provided.	Dye removal was maximum under strongly acid pH (0.7–2). Dye removal decreased with increasing ionic strength at 0.2 mol NaCl. Electrostatic interactions between dye and PUF dominated dye removal. Dye sorption obeyed S-type isotherm mode sq_{max}: 49 µmol/g for E-124, and 2 µmol/g for E-143	Tikhomirova et al., 2018
PUF	Direct Red 80 (DR80) and Reactive Blue 21 (RB21)	Batch experiments using concentrations 10–60 mg/L. Column experiment low rates were 2.5, 7.5, 12.5, and 17.5 mL/min, while concentrations were 10, 15, 20, 30, 40, 50 and 60 mg/L.	Data obeyed Langmuir model (r^2 =0.98). $q_{max:}$ 4.50 mg/g (DR80), 8.31 mg/g (RB21). Flow rate less than 2.5 mL/min achieved high removal but slowed the experiment due to non-feasible retention times, while flow rates exceeding 17.5 mL/min provided less contact time between adsorbent and dye, thus reducing removal efficiency. High initial dye concentrations in a fixed bed with a flow rate of 7.5 mL/min reduced removal off both dyes due to reduced availability of adsorption sites. A removal of 80% was achieved under optimized experimental conditions done using response surface methodology.	Neta et al., 2011
Bio–based PU/chitosan foam (PU/chitosan)	Food red 17	Batch experiments at concentration 25 mg/L, pH 2 and temperature of 328 K	Removal: > 98%	Da Rosa Schio et al., 2019)
Polyether-based PUF	Four food dyes: Sunset Yellow, Tartrazine, Ponceau 4R, Fast Green FCF	Batch experiments	Maximum adsorption occurred pH 2 with removal of 20–30% except Fast Green FCF whose removal was maximum at pH 8.0. Electrostatic interactions including ion exchange were responsible for adsorption under acidic pH, and hydrophobic interactions for dyes with benzene rings	Ramazanova et al., 2013
Organic pollution and petroleum hydrocarbons:				
Rhodococcus sp. F92 immobilized on PUF	Four petroleum products: crude Arabian light, crude Al-Shaheen, diesel, and oil slops	Batch cultures with synthetic sea water supplemented with N and P: 23.4 g/L NaCl, 0.75 g/L KCl, 7 g/L MgSO4 Æ7H2O, 0.67 g/L $CaCl_2.2H_2O$, 0.001 g/L $FeSO_47H_2O$, 70 g/L K_2HPO_4, 30 g/L KH_2PO_4 and 100 g/L NH_4NO_3. Final pH: 7.5. N and P solutions prepared individually and added just prior to use.	*Rhodococcus* sp. F92 was effectively immobilized viable cell s (10^9 cells/cm^3 PUF, maximum attachment efficiency: 90%. Immobilized F92 cells degraded about 90% of total n-alkanes in 1 week (30 °C).	Quek et al., 2006
PUF impregnated with lignin LPUF)	Crude oil	Batch experiments used to test effect of concentration (10–200 g/L) and isotherm models at room temperature on sole PUF and LPUF.	Lignin reduced hydrophobicity and increased oil adsorption by 35.5 relative to sole PUF. Data obeyed Langmuir isotherm model with q_{max} of 28.9 g/g Adsorption was spontaneous with change in Gibb's free energy of − 4.4 kJ/mol. 95% removal achieved after five regeneration cycles.	Santos et al., 2017
Microorganisms (B350) immobilized in PU (IPU) foam and sole PU	COD	Packed bed column experiment operated in a batch-wise mode was also conducted to test removal of organic pollution (COD) using synthetic wastewater (270 mg $C_6H_{12}O_6$, 18.5 mg $CuSO_4$, 20 mg NH_4Cl, and 10 mg KH_2PO_4)	Column data showed that COD concentrations dropped from 270 mg/L to 55 mg/L within the first 4 h, giving removal efficiencies of 80%	Zhou et al., 2009
Indolocarbazole based polymer coated PUF	Organic solvents/oil	Batch experiments to determine adsorption ion capacity and isotherms	Adsorption capacity: 100–240 g/g. Fast and selective removal observed. Adsorbents were reusable 50 times mechanical squeezing with structural deformation. Data obeyed Langmuir isotherm model.	Vintu and Unnikrishnan, 2019
PU cross-linked pine cone	2-nitrophenol			Kupeta et al., 2018
Cross-linked CD PU copolymerized with functionalised multiwalled	Trichloroethylene (TCE)	Packed column experiment at various concentrations (10 mg/L and 10 µg/L) at flow rate 3–5 mL/min.Regeneration done using 10 mg/L *p*-nitrophenol.	PUF polymers with MWCNTs removed achieved about 100% removal of TCE but the chromatogram of native polymers had residual TCE peak. PUF polymer with	Salipira et al., 2008a,2008b

(*continued on next page*)

Table 4 (*continued*)

Adsorbent	Contaminants	Experimental conditions	Results	References.
carbon nanotubes (MWCNTs)			MWCNTs lost 5% of its mass after 9 cycles compared to 17% for native polymer.	
Emerging contaminants:				
β-CD−Ionic Liquid PU-functionalized magnetic adsorbent	Two perfluorinated compounds (perfluorooctanesulfonate (PFOS), perfluorooctanoic acid (PFOA))	Batch experiments used to study kinetics, isotherms, removal capacity, and regeneration.	Sorption equilibrium for PFOS, and PFOA reached within 4, and 6 h. Data followed pseudo-second-order kinetic model. pH effect more pronounced for PFOA than PFOS. Adsorption isotherms showed that the heterogeneous sorption capacities were 13,200 and 2500 μg/g for PFOS and PFOA. Reduction in POFCs adsorption observed in Cr(VI)-PFC binary sorption studies, but Cr(VI) removal was independent of PFCs as co-pollutants. PFCs removal occurred via electrostatic and hydrophobic interactions. Adsorbents were recovered using an external magnet, regenerated, and reused in at least 10 cycles without significant reduction in efficiency.	Badruddoza et al., 2017
gamma-cyclodextrin PU polymer (GPP), gamma-cyclodextrin/starch PU copolymer (GSP), starch PU polymer (SPP)	Dialkyl phthalates (dimethyl phthalate (DMP) and diethyl phthalate (DEP)	Batch experiments to determine removal capacity and isotherms	Data fitted L-isotherms and obeyed both Langmuir and Freundlich models. Adsorption was spontaneous and driven by enthalpy change. Removal occurs via multiple adsorbent–adsorbate interactions including hydrogen bonding, – stacking, and pore-filling.	Okoli et al., 2014
Insoluble nanoporous CD polymers were synthesized using bifunctional isocyanate linkers.	Chlorinated disinfection by-products (DBPs) and odor-causing compound (2–methylisoborneol (2–MIB)).	Batch experiments at varying concentrations	CD polymers showed excellent absorption efficiency (>99%) higher than granular activated carbon. CD has had regeneration potential	Mhlanga et al., 2007

that removal was higher for cationic (malachite green) (75%) than anionic dye (methyl orange) (<10%) after 120 min. In the same study, thermodynamic modeling showed that the adsorption process was endothermic and occurred spontaneously. The adsorption data obeyed the following models: (1) pseudo second-order kinetics, and (2) Langmuir isotherm with a maximum adsorption capacity of 80 mg/g (Kumari et al., 2016). Following regeneration, the LPUF adsorbent was reusable, giving a cumulative adsorption capacity of 1.33 g/g after 20 cycles. Other dyes studies, nature of PUF adsorbents used, and removal mechanisms are summarized Table 4. However, as discussed for other contaminants, the behavior and fate of dyes, including degradation products are not reported in these studies. Therefore, it is unclear in current studies whether dyes are simply remove from liquid to solid phase or undergo biochemical degradation.

6.3. *Organic pollution and petroleum hydrocarbons*

A few studies have used PUF-based materials in cultures for the removal of organic pollution and petroleum hydrocarbon products in aqueous systems (Table 4). For example, Zhou et al. (2009) used fixed-bed packed column containing microorganisms (B350) immobilized in polyurethane (IPU) foam and sole polyurethane (PU) for the removal of chemical oxygen demand (COD) in synthetic wastewater. The results showed COD concentration for the IPU dropped from 270 mg/L (initial concentration) to 55 mg/L (final concentration) within 4 h, corresponding to a removal efficiency of 80%. The removal of COD by IPU was about double that of sole PU.

Polyurethane foam impregnated with lignin (LPUF) removed 35.5% more crude oil than sole PUF (Santos et al., 2017). Lignin increased adsorption of crude oil by reducing its hydrophobicity. The adsorption process was best described by the Langmuir isotherm model (maximum adsorption capacity: 28.9 g/g). A negative change in Gibb's free energy ($\Delta G = -4.4$ kJ/mol) was observed, indicating a spontaneous adsorption process. Regeneration studies showed that the recycled LPUF could remove 95% of the crude oil even after five regeneration cycles.

In one study, *Phodococcus* spp. F92 was effectively immobilized on PUF, giving a 90% maximum attachment efficiency equivalent to 10^9 viable cells per cm^3 of PUF (Quek et al., 2006). The immobilized F92 cells degraded about 90% of the total n-alkanes in four petroleum products (i.e., diesel, oil slops, Arabian light crude (ALC), Al-Shaheen crude (ASC)) within 1 week at 30 °C. In another study, indolocarbazole based polymer coated super-adsorbent polyurethane sponges were shown to have rapid and selective removal of oils and organic solvents as evidenced by adsorption capacities ranging from 100 to 240 g/g. The adsorption process occurred according to the Langmuir isotherm model. In the same study, the adsorbents were regenerated 50 times by mechanical squeezing without loss of structural stability. However, there is a lack of data on the behavior, and fate of organic pollution and petroleum hydrocarbons adsorbed on PUF adsorbents, and their associated human and ecological health risks.

6.4. *Synthetic pesticides*

Polyurethane-based adsorbents have been applied to remove synthetic pesticides such as organochlorines, and atrazines or triazines such as 2,4-bis(Isopropylamino)-6-methylthio-s-triazine also known as prometryn. Prometryn is a post-or pre-emergence herbicide belonging to sulfur-substituted, thiomethyl or thio-S(symmetrical)-triazines, which are used as pre-or post-emergence herbicides (Đikić, 2014). For example, a tannic acid azo polyurethane (PUF–azo–Tan) adsorbent was applied in batch experiments for the removal of prometryn and atrazine in water (Moawed et al., 2015). The adsorption capacity of PUF–azo–Tan was 32 mg/g equivalent to 0.14 mmol/g and the adsorption occurred within 3–5 min. Kinetic and isotherm modeling showed that the adsorption data obeyed the pseudo-second-order ($r^2 = 0.989$) and Freundlich isotherm ($r^2 = 0.993$), respectively (Moawed et al., 2015).

Acid modified polyurethane foam was use to remove 99–100% of organochlorine pesticides from wastewater (Moawed and Radwan, 2017). The adsorbent was regenerated over 30 cycles without losing its adsorption capacities. A polyurethane foam loaded with sodium dodecylsulfate (SDS) was used to cationic 'quat' or paraquat pesticides (paraquat, diquat, difenzoquat) from aqueous solution (Vinhal et al., 2017). Results showed more than 90% removal, and the adsorption process was best described by a pseudo second-order kinetic model.

The capacity of two PUF adsorbents to remove a pesticide Chlorpyrifos was investigated in fixed-bed column experiments packed with: (1) silver nanoparticles coated onto PUF (CPUF), and (2) silver nanoparticles fused into PUF (FPUF). The results showed that, at a flow rate of 20 mL/h a maximum removal efficiencies of 92–94% for CPU, and 90–96 for FPU were observed. Removal efficiencies and breakthrough times decreased with increasing flow rate of the pesticide-contaminated inflow water. However, it is unclear whether the removal from aqueous solution is accompanied by degradation of the pesticides into less toxic or benign by-products.

6.5. Emerging organic contaminants

In recent years, PUF-based adsorbents have been used for the remediation of emerging contaminants in water (Table 4). Emerging contaminants include personal care products, pharmaceuticals, illicit drugs, industrial solvents, endocrine disrupting compounds, and disinfection by-products, among others. Badruddoza et al. (2017) developed β-cyclodextrin−ionic liquid PUF- modified magnetic adsorbent and applied it to remove two perfluorinated compounds (PFCs): (1) perfluorooctanoic acid (PFOA), and (2) perfluorooctane sulfonate (PFOS). The adsorption equilibria of PFOA and PFOS were reached within 6 h and 4 h, respectively. Adsorption process was best described by the pseudo-second-order kinetic model (Badruddoza et al., 2017). The effect of solution pH was more pronounced for PFOA than PFOS. Adsorption isotherms showed that the heterogeneous sorption capacity was 13, 200 μg/g for PFOS and 2500 μg/g for PFOA. In binary solution of Cr(VI) and PFCs, the adsorption of PFCs was reduced, but Cr(VI) removal was independent of the presence of co-contaminants (PFCs). PFCs removal occurred via both electrostatic attraction and hydrophobic interactions. The adsorbents were recovered using a permanent magnet, and they retained their adsorption capacity even after regeneration and reuse for more than 10 times.

In batch experiments, Okoli et al. (2014) investigated the removal of two dialkyl phthalates (diethyl phthalate, DEP, and dimethyl phthalate, DMP) using three PUF adsorbents: (1) starch PUF polymer (SPP), (2) gamma-cyclodextrin/starch PUF copolymer (GSP), and gamma-cyclodextrin PUF polymer (GPP). The adsorption process followed both the Freundlich and Langmuir isotherm models. Thermodynamic analysis showed that adsorption was spontaneous, driven by changes in enthalpy. Contaminant removal occurred via multiple adsorbent–adsorbate interactions including pore filling, hydrogen bonding, and stacking.

In one study, odor-causing compound (2–methylisoborneol (2–MIB)) and chlorinated disinfection by-products (DBPs) were removed using insoluble nanoporous cyclodextrin (CD) polymers synthesized using bifunctional isocyanate linkers (Mhlanga et al., 2007). The adsorption efficiency of the CD polymers (>99%) were higher than that of granular activated carbon. CD showed a high regeneration capacity. Given that emerging contaminants represent a diverse group of chemicals, several such contaminants are still under-studied.

To this point, several PUF adsorbents have been developed and applied to remove a wide range of contaminants in aqueous systems (Table 2). The removal capacities are largely high, and the kinetics rapid. As more emerging pollutants emerge, PUF is likely to be an important adsorbent in water treatment systems. However, on the one hand, limited comparative studies exist on the adsorption capacity and selectivity of the various PUF adsorbents. On the other hand, a direct comparison of the adsorption capacities and selectivity of the various adsorbents towards different types of contaminants among studies is problematic. This is because the operating conditions (e.g., agitation rate) and even solution chemistry (e.g., pH, initial contaminant concentrations, interfering solutes) vary considerably among studies. Therefore, systematic comparative studies are required in order to identify the best performing PUF adsorbents for the removal of various contaminants.

A close examination of the studies investigating the effects of various preparation methods and operating conditions revealed that the bulk of the studies investigated one factor independent of the other factors. Therefore, such studies fail to provide information of the optimum combination of the various factors. Hence, further studies using optimization tools such as response surface methodology are required to determine the optimum combination of the factors for the preparation and operating conditions for the various PUF adsorbents.

6.6. A summary comparison of PUF adsorbents to other biopolymers/polymers

A wide range of precursor materials, and synthesis/modification methods are used for the preparation of organic and synthetic adsorbents. This gives a wide range of organic and synthetic adsorbents with varying properties and contaminant adsorption capacities. Given this large diversity, a comprehensive comparison of PUF adsorbents to other organic and synthetic adsorbents is beyond the scope of the current study. Here, a summary comparison of PUF adsorbents to a few selected organic adsorbents with high contaminant adsorption capacities is presented.

PUF adsorbents can be classified among a broad group of biopolymer/polymer adsorbents. These biopolymer/polymer adsorbents include: (1) carbohydrate and cellulose biopolymers, (2) chitosan-based composites, (3) biopolymer-clay composites, and (4) alginate-based composites (Khademian et al., 2020). For brevity, a detailed comparison of PUF adsorbents to other biopolymer/polymer adsorbents is beyond the scope of the present review. In fact, a number of reviews exist on the preparation, properties and performance of biopolymer/polymer adsorbents (Karimi-Maleh et al., 2021; Khademian et al., 2020). Similar to PUF adsorbents, biopolymer/polymer adsorbents are generally characterized by high adsorption capacity relative to conventional adsorbents such as activated carbon. For example, a high adsorption capacity of 636.6 mg/g has been reported for a magnetic chitosan biopolymer (Chen et al., 2020). This value is more than two times the adsorption capacity of methyl orange (255 mg/g) reported for polyurethane-polyaniline macroporous foam (Mendieta-Rodriguez et al., 2021). For Cu^{2+}, an adsorption capacity of 131.16 mg/g has been reported on a biopolymer composite prepared from cellulose nanocrystals derived from almond (*Prunus dulcis*) shell (Maaloul et al., 2021). In the same study, the adsorption data was reported to obey the Dubinin-Radushkevich model, and the Elovich kinetic model. This suggests that Cu^{2+} adsorption was mainly attributed to the chemisorption occurring on the heterogeneous surface of the adsorbent, while thermodynamic data showed that the process was endothermic and spontaneous (Maaloul et al., 2021).

A number of studies, including reviews, exist on the regeneration and reusability of biopolymer/polymer adsorbents (Chen et al., 2020; Karimi-Maleh et al., 2021; Khademian et al., 2020; Maaloul et al., 2021; Narayanan et al., 2020; del Mar Orta et al., 2020). Depending on the nature of the biopolymer/polymer adsorbents and the contaminants to be eluted, regeneration of biopolymer/polymer adsorbents using chemicals (EDTA, HCl, acetone, etc) similar to those for PUF adsorbents (Section 7) have been reported (Khademian et al., 2020; Maaloul et al., 2021). Similar to PUF adsorbents, biopolymer/polymer adsorbents can also be regenerated using thermal methods (Narayanan et al., 2020). Chen et al. (2020) used a magnetic method to regenerate magnetic chitosan (CS)-Fe_3O_4 composite (Fe_3O_4-CS) after the adsorption of methyl orange. A number of generic methods used to prepare biopolymer/polymer adsorbents such as magnetic and metal/metal oxide composites may be extended to the preparation of the corresponding

PUF adsorbents. In this regard, the regeneration techniques such as magnetic separation used for such biopolymers/polymers (e.g., magnetic composites) may also be applied to their corresponding PUF counterparts.

Relative to biopolymers such as chitosan and cellulose, PUF is not easily biodegraded. Thus spent PUF adsorbents persist in the environment and pose environmental and human health risks. Fortunately, the mechanical properties of PUF allow for its use in a number of structures to prolong the life-span. At the end of the life cycle however, the PUF will still require appropriate disposal following an environmental impact assessment to reduce the risk to the environment. To achieve this, a lifecycle analysis could be useful, and this is an area that deserves further research.

Notably, the available data on contaminant removal mechanisms, adsorption capacity, and kinetic and isotherm modeling do not allow a direct comparison of PUF adsorbents to other biopolymers/polymers. This is due to confounding effects arising from differences in the precursor materials, isotherm and kinetic models tested, preparation methods, operating conditions, and solution chemistry. Therefore, systematic comparative studies using similar preparation methods, contaminants, isotherm and kinetic models, operating conditions, and regeneration methods are still needed. Such comparative information is crucial in the choice of biopolymer/polymer adsorbents for various remediation applications. Moreover, the application of PUF-based adsorbents towards the removal of multi-component pollutants in real wastewaters is a challenging task that requires further investigation.

7. Regeneration, recycling and disposal of spent polyurethane adsorbents

The bulk of the available data on the application of polyurethane adsorbents for the remediation of contaminants in aqueous systems are limited to laboratory-scale experiments. Such studies often exclude key aspects pertaining to the large-scale application and adoption of adsorbents. These aspects include: (1) feasible methods for the regeneration and recycle the adsorbents at scale relevant to industrial applications, (2) final disposal of contaminant-laden spent adsorbents. Therefore, the potential for regeneration, recycling, and the disposal of the spent adsorbents are discussed in this section.

7.1. Regeneration methods

In general, several methods can be used for the regeneration of spent adsorbents. These methods include: (1) chemical methods (e.g., use of acids, alkaline solutions), (2) mechanical methods (e.g., filtration, squeezing, decanting) (Centenaro et al., 2017; Amorim et al., 2021; Anju and Renuka, 2020), and thermal methods. Unique to PUF however, is the capability for regeneration by simple mechanical means such as squeezing. This is mainly due to the intrinsic spongey nature of PUF, which permits considerable size reduction and releases the adsorbed pollutants upon the application of a compressive force. As a result, PUF adsorbents have been regenerated for reuse over a larger number of cycles relative to biopolymer adsorbents. However, comparative studies investigating the regeneration potential of polyurethane adsorbents versus biopolymers/polymers using various methods are still limited. Moreover, the socio-economic and technical feasibility of the various regeneration methods are poorly studied. The lack of data on the regeneration potential of various polyurethane adsorbents could limit the large scale uptake, adoption, and application of PUF adsorbents.

7.2. Recycling and disposal of spent polyurethane adsorbents

(1) **Novel construction materials**

Polyurethane has a number of unique properties including high porosity, low density, high thermal and acoustic insulation, and low thermal conductivity. Thus, scope exists to develop novel construction materials incorporating spent polyurethane-based adsorbents and waste polyurethane. In this regard, PUF can be used as an ideal additive or filler material in novel construction materials possessing high acoustic and thermal insulation properties. However, evidence on this application of post-consumer polyurethane is still lacking.

(2) **Polyurethane-based outdoor furniture**

Polyurethane tends to be highly stable under typical environmental exposure, including harsh weather such as rainfall, and extreme ambient air temperatures. Therefore, a potential exist to use post-consumer polyurethane as filler material in outdoor furniture such as park and garden chairs. This potential application is motivated by the widespread use of polyurethane for household furniture production. Research is needed to develop and evaluate outdoor furniture incorporating post-consumer polyurethane, including technical behavior, stability under ambient conditions, and consumer perceptions and attitudes towards such products.

(3) **Polyurethane-based dual remediation systems**

The available evidence on polyurethane adsorbents is limited to contaminant remove via a single process (i.e., adsorption). In the case of metal-laden spent adsorbents scope may exist for the in-situ development of polyurethane based dual remediation systems. In the case or organic contaminants, and even some inorganic ones, there is a possibility to harness both adsorption, and subsequently biochemical degradation of the contaminant. Hence, conceptually, the development of a dual systems coupling adsorption to biochemical degradation is a potential research area. In such dual systems, adsorption can be used to increase the residence time of the contaminants in the system being remediated in order to increase the subsequent removal efficiency via biochemical degradation. Dual systems based on this concept may include polyurethane adsorbent-metal(oxide) catalysts, where contaminant removal occurs on both the adsorbent matrix and the catalyst. The unanswered question is whether spent adsorbents can be regenerated to recover valuable materials, and then recycle the polyurethane to develop dual remediation systems. Alternatively, in the case of polyurethane adsorbent-metal(oxide) composites, can such novel materials be synthesized in situ using metal-laden spent adsorbents. The in-situ development of the dual adsorbent-metal(oxide) composites require further studies especially in cases where the spent adsorbents are enriched in transition and rare earth elements with known catalytic activity. The dual remediation system is potentially interesting in the context of organic contaminants such as dyes and pesticides, and emerging ones such as pharmaceuticals, endocrine disruption compounds, personal care products, and even antimicrobial resistance.

Relative to biopolymers such as chitosan and cellulose, PUF is not easily biodegraded. Thus spent PUF adsorbents persist in the environment and pose environmental and human health risks. Fortunately, the mechanical properties of PUF allow for its use in a number of structures to prolong the life-span. At the end of the life cycle however, the PUF will still require appropriate disposal following an environmental impact assessment to reduce the risk to the environment. To achieve this, a lifecycle analysis could be useful, and this is an area that deserves further research.

7.3. Behavior and fate of contaminants on spent polyurethane adsorbents

Adsorption as a remediation technology has a number of potential limitations, among them, the fact that the process transfers contaminants from the dissolved aqueous phase to a solid or adsorbed phase (Gadd et al., 2009). Thus, barring the change in phase, in most cases, the contaminants do not undergo biochemical breakdown. Therefore, the behavior, fate, and health risks of the contaminant-laden spent PUF adsorbents remain poorly understood. For example, one may wonder whether the contaminants are later released back into the dissolved phase as the spent adsorbents age or they undergo natural physical and biochemical degradation to less toxic forms. Currently, it is also unclear whether the adsorbed contaminants are less bioavailable, bioaccessible and less toxic than the dissolved phase of the contaminants. This highlights the need to understand the behavior, fate, and human and ecological health risks of spent adsorbents and their associated contaminants.

8. Future perspectives and research directions

The foregoing discussion points to several potential avenues for future research on the development, application, regeneration and recycling, and potential health risks.

(1) **Synthesis and characterization**
The synthesis and characterization of novel materials including polymer catalyst, and adsorbent-catalyst dual systems is an emerging and fast-developing area of research. Hence there is need to further investigate synthesis methods including facile ones for novel polyurethane adsorbents, catalysts, and even dual systems, and the subsequent detailed characterization of such novel materials. Such studies should also investigate the contaminant removal mechanisms, including reaction kinetics, thermodynamics, and isotherm modeling. Besides single-contaminant systems, such studies should complex aqueous systems (binary, ternary, quaternary etc) in order to better understand potential interference among contaminants, including possible synergistic and antagonistic interactions. Recent advances in analytical methods such as hyphenated methods, in-situ and solid state techniques can be used to better understand the nature and behavior of such novel materials.

(2) **Removal of microbial contaminants**
The removal of microbial contaminants such as human pathogens and other biotoxins such as antimicrobial resistance and their resistance genes were beyond the scope of the present review. Therefore, further research is required to understand the removal capacity, behavior and fate of microbial contaminants and antimicrobial resistance by PUF adsorbents. In light of the on-going COVID-19 pandemic, such future studies should including (re)-emerging viral pathogens such as SARS-CoV-2 and their surrogates.'

(3) **Industrial applications**
The available data on the application of polyurethane adsorbents is limited to just a few contaminants including metals, and conventional organic contaminants (e.g., dyes, pesticides). The capacity of such adsorbents to remove a large number of emerging contaminants is yet to be investigated. Emerging contaminants is an emerging health issue that has received global public and research attention in both developed and developing countries (Gwenzi and Chaukura, 2018; Gwenzi et al., 2020). Hence, research is required to address this gap. Research on industrial applications should also address the technical, and socio-economic feasibility of large-scale application of such technology, and even consumer and public perception and attitudes.

(4) **Regeneration recycling of spent adsorbents**
Further research is required to investigate the most appropriate and cost effective methods for regenerating polyurethane adsorbents. Further research is also need to understand the physicochemical and mechanical stability and adsorption performance of recycled PUF adsorbents and catalysts with respect to: (1) contaminant removal and mechanisms involved, (2) loss of reactivity including catalyst poisoning, and (3) mechanical and thermal degradation. Moreover, the various potential recycling options highlighted require further research including the development, and evaluation of pilot systems, and public and consumer perceptions and attitudes. Comparative studies with other existing competing technologies are needed to facilitate uptake and adoption.

(5) **Fate, behavior, and health risks of spent PUF adsorbents**
Research is needed to investigate the following aspects with respect to contaminant-laden adsorbents: (1) speciation, bioavailability and bioaccessibility of contaminants, (2) quantitative ecotoxicological studies based on dose-response relationships using a battery of ecotoxicological tests, and environmentally relevant concentrations and even mixtures of spent adsorbents and other health stressors and typical co-contaminants. It is currently unclear whether contaminant-laden spent adsorbents pose less human and ecological health risks than their dissolved counterparts. Furthermore, the health risks posed by the polyurethane adsorbents and associated post-consumer products are still poorly understood. This calls for further research to address these gaps.

(6) **Environmental footprinting of polyurethane adsorbents**

Compared to narrow studies focusing on one aspect or point in the life cycle of a product, life cycle analysis is a powerful tool for gaining a comprehensive understanding of environmental footprints. Studies on the environmental footprints of polyurethane adsorbents and recycled products are still lacking. Thus, comparative environmental footprinting studies of the energy, water, carbon, and social impacts of polyurethane adsorbents relative other adsorbents are required. Such studies should use life cycle analysis approaches. Due to their environmental persistence, PUF adsorbents may cause environmental health risks and visual impacts for a long time. To address this limitation, a number of technologies for converting spent PUF adsorbents to value-added industrial materials were proposed.

9. Conclusions and outlook

The present comprehensive review investigated the preparation, properties, and applications of PUF based adsorbents for the remediation of organic and inorganic pollutants, including emerging contaminants in aqueous systems. The synthesis approaches, and physicochemical properties of polyurethane related to its industrial applications were presented. PUF has several industrial applications as cushion material in packaging, bedding, automotive interiors, furniture, and carpet underlay, among others. However, due to its bulkiness and environmental resilience, the disposal of post-consumer polyurethane poses significant health risks. Thus, the development and applications of polyurethane adsorbents is a novel option to reduce the environmental impacts of post-consumer polyurethane, while simultaneously remediating aquatic pollution. Several PUF-based adsorbents have been developed including those with immobilized (micro)organisms, composites such as lignin-PUF, and chitosan-PUF, among others. PUF adsorbents effectively remove metals, metalloids, rare earth elements, synthetic organic pesticides (atrazines, organochlorines, and triazines), organic pollution (COD), petroleum hydrocarbon products, emerging contaminants (e.g., disinfection by-products, perfluorinated compounds, and industrial dyes. The contaminants removal mechanisms related to the adsorption data fitting to adsorption isotherm and kinetic models, thermodynamic analysis were discussed. Depending on the charge and structure of the contaminants, removal occurred via multiple-adsorbent-adsorbate interactions including electrostatic interactions, ion exchange, and hydrophobic interactions, among others. The role of adsorption operating conditions such as pH, contact time, ligand concentrations, ionic strength, and initial contaminant concentrations were discussed. To explore the sustainable use of PUF based adsorbent in contaminant removal, the discussions related to regeneration methods, options for the recycling and final disposal of spent adsorbents were presented, including use in novel construction materials, and outdoor furniture. Finally, several knowledge gaps were formulated to guide future research.

Declaration of Competing Interest

The authors declare that they have no known competing financial interests or personal relationships that could have appeared to influence the work reported in this paper.

Acknowledgments

Dr. Rangabhashiyam S acknowledges SASTRA Deemed University for sanctioning TRR research scheme.

References

Abdelrahman, J., Rem, B., Abdelbaki, S.N., Mustafa, M.B.A., Muneer, E.N., Muftah, W. M., Abdul, 2020. Adsorption of organic pollutants by nanomaterial-based adsorbents: an overview. J. Mol. Liq. 301, 112335.
Abhijit, D., Prakash, M., 2020. A brief discussion on advances in polyurethane applications. Adv. Ind. Eng. Polym. Res. 3, 93–101.
Ahmad, D., Hamish, R.M., Gordon Mc, K., Ahmed, A., 2016. Removal of emulsified and dissolved diesel oil from high salinity wastewater by adsorption onto graphene oxide. J. Environ. Chem. Eng. 7, 103106.
Akeem, A.O., Mustafa, G., 2015. Microwaves initiated synthesis of activated carbon-based composite hydrogel for simultaneous removal of copper(II) ions and direct red 80 dye: a multi-component adsorption system. J. Taiwan Inst. Chem. Eng. 47, 125–136.
Akindoyo, J.O., Beg, M.D.H., Ghazali, S., Islam, M.R., Jeyaratnam, N., Yuvaraj, A.R., 2016. Polyurethane types, synthesis and applications —A review. RSC Adv. 6, 114453–114482.
Alhkawati, M.S., Banks, C.J., 2004. Removal of copper from aqueous solution by Ascophyllum nodosum immobilised in hydrophilic polyurethane foam. J. Env. Man. 72 (4), 195–204.
Ali, A., Ramin, N., Simin, N., Amir, H.M., Ali, R.M., 2020. Comprehensive systematic review and meta-analysis of dyes adsorption by carbon-based adsorbent materials: classification and analysis of last decade studies. Chemosphere 250, 126238.
Alhakawati, M.S., Banks, C.J., 2004. Removal of copper from aqueous solution by Ascophyllum nodosum immobilised in hydrophilic polyurethane foam. J. Environ. Manage. 72 (4), 195–-204.
Amorim, F.V., Padilha, R.J.R., Vinhas, G.M., Luiz, M.R., de Souza, N.C., de Almeida, Y.M. B., 2021. Development of hydrophobic polyurethane/castor oil biocomposites with agroindustrial residues for sorption of oils and organic solvents. J. Colloid Interface Sci. 581, 442–454.
Anju, M., Renuka, N.K., 2020. Magnetically actuated graphene coated polyurethane foam as potential sorbent for oils and organics. Arab. J. Chem. 13, 1752–1762.
Badruddoza, A.Z.M., Bhattarai, B., Suri, R.P., 2017. Environmentally Friendly β-cyclodextrin–ionic liquid polyurethane-modified magnetic sorbent for the removal of PFOA, PFOS, and Cr (VI) from water. ACS Sustainable Chem. Eng 5 (10), 9223–9232.
Baker, J.W., Haldsworth, 1947. 135. The mechanism of aromatic side-chain reactions with special reference to the polar effects of substituents. Part XIII. Kinetic examination of the reaction of aryl isocyanates with methyl alcohol. J. Chem. Soc. 713.
Baker, J.W., Davies, M.M., Gaunt, J., 1949. 5. The mechanism of the reaction of aryl isocyanates with alcohols and amines. Part IV. The evidence of infra-red absorption spectra regarding alcohol–amine association in the base-catalysed reaction of phenyl isocyanate with alcohols. J. Chem. Soc. 0, 24–27.
Barroso-Solares, S., Merillas, B., Cimavilla-Roman, P., Rodriguez-Perez, M.A., Pinto, J., 2020. Enhanced nitrates-polluted water remediation by polyurethane/ sepiolite cellular nanocomposites. J. Clean. Prod. 254, 120038.
Belenguer-Sapiña, C., Pellicer-Castell, E., Amorós, P., Simó-Alfonso, E.F., Mauri-Aucejo, A.R., 2020. A new proposal for the determination of polychlorinated biphenyls in environmental water by using host-guest adsorption. Sci. Total Environ. 724, 138266.
Burkus, J., 1961. Tertiary amine catalysis of the reaction of phenyl isocyanate with alcohols. J. Org. Chem. 26 (3), 779–782.
Centenaro, G.S.N.M., Facin, B.R., Valério, A., de Souza, A.A.U., da Silva, A., de Oliveira, J.V., de Oliveira, D., 2017. Application of polyurethane foam chitosan-coated as a low-cost adsorbent in the effluent treatment. J. Water Process Eng. 20, 201–206.
Chen, B., Long, F., Chen, S., Cao, Y., Pan, X., 2020. Magnetic chitosan biopolymer as a versatile adsorbent for simultaneous and synergistic removal of different sorts of dyestuffs from simulated wastewater. Chem. Eng. J. 385, 123926.
Chen, X., Zhou, H., Li, Y., 2019. Effective design space exploration of gradient nanostructured materials using active learning based surrogate models. Mater. Des. 183, 108085.
Clares, M.E., Guerrero, M.G., García-González, M., 2015. Cadmium removal by Anabaena sp. ATCC 33047 immobilized in polyurethane foam. Inter. J. Environ. Sci. Techno. 12 (5), 1793–1798.
Coady, D.J., Horn, H.W., Jones, G.O., Sardon, H., Engler, A.C., Waymouth, R.M., Rice, J. E., Yang, Y.Y., Hedrick, J.L., 2013. Polymerizing base sensitive cyclic carbonates using acid catalysis. Macro Lett. 2 (4), 306–312.
Coutelier, O., El Ezzi, M., Destarac, M., Bonnette, F., Kato, T., Baceiredo, A., Sivasankarapillai, G., Gnanou, Y., Taton, D., 2012. N-Heterocyclic carbene-catalysed synthesis of polyurethanes. Polym. Chem. 3 (3), 605–608.
de Almeida, G.N., de Sousa, L.M., Netto, A.D.P., Cassella, R.J., 2007. Characterization of solid-phase extraction of Fe(III) by unloaded polyurethane foam as thiocyanate complex. J. Colloid Interface Sci. 315, 63–69.
da Rosa Schio, R., da Rosa, B.C., Goncalves, J.O., Pinto, L.A.A., Mallmann, E.S., Dotto, G. L., 2019. Synthesis of bio-based polyurethane/chitosan composite foam using ricinoleic acid for the adsorption of food red 17 dye. Int. J. Biol. Macromol. 121, 373–380.
del Mar Orta, M., Martín, J., Santos, J.L., Aparicio, I., Medina-Carrasco, S., Alonso, E., 2020. Biopolymer-clay nanocomposites as novel and ecofriendly adsorbents for environmental remediation. Appl. Clay Sci. 198, 105838.
Dias, M.A., Lacerda, I.C.A., Pimentel, P.F., De Castro, H.F., Rosa, C.A., 2002. Removal of heavy metals by an Aspergillus terreus strain immobilized in a polyurethane matrix. Letters App. Microbiol. 34 (1), 46–50.
Dixit, A., Dixit, S., Goswami, C.S., 2011. Process and plants for wastewater remediation: a review. Sci. Rev. Chem. Commun. 11, 71–77.
Dikić, D., 2014. Prometryn. In Encyclopedia of Toxicology, 3. Elsevier Inc., Academic Press, pp. 1077–1081.
Dutta, V., Sheetal, Pankaj, R., Ahmad, H.B., Jyotsana, K., Pardeep, S., 2020. Fabrication of visible light active $BiFeO_3$/CuS/SiO_2 Z-scheme photocatalyst for efficient dye degradation. Mater. Lett. 270, 127693.
Eibagi, H., Faghihi, K., Komijani, M., 2020. Synthesis of new environmentally friendly poly(urethane-imide)s as an adsorbent including β-cyclodextrin cavities and attached to iron nanoparticles for removal of gram-positive and gram-negative bacteria from water samples. Polym. Test. 90, 106734.
Esperanza, D., Salvador, B.M., Carmen, H., Lucía, C., Beatriz, G., 2019. Optimizing a low added value bentonite as adsorbent material to remove pesticides from water. Sci. Total Environ. 672, 743–751.
Fallah, Z., Isfahani, H.N., Tajbakhsh, M., 2019. Cyclodextrin-triazole-titanium based nanocomposite: preparation, characterization and adsorption behavior investigation. Process Saf. Environ. Prot. 124, 251–265.
Faysal, M.D.H., Nasrin, A., Yanbo, Z., 2020. Recent advancements in graphene adsorbents for wastewater treatment: current status and challenges. Chin. Chem. Lett. https://doi.org/10.1016/j.cclet.2020.05.011.
Fernández, C.E., Bermúdez, M., Versteegen, R.M., Meijer, E.W., Vancso, G.J., Muñoz-Guerra, S., 2010. An overview on 12-polyurethane: synthesis, structure and crystallization. Eur. Polym. J. 46, 2089–2098.
Fisch, K.C., Rumao, L.P., 1970. Catalysis in isocynate reactions. J. Macromol. Sci. Part C Polym. Rev. 5, 103–149.
Foo, K.Y., Hameed, B.H., 2010. Detoxification of pesticide waste via activated carbon adsorption process. J. Hazard. Mater. 175, 1–11.
Gadd, G.M., 2009. Biosorption: critical review of scientific rationale, environmental importance and significance for pollution treatment. J. Chem. Techno. Biotechno.: Inter. Res. Proc. Environ. Clean Techno. 84 (1), 13–28.
Georgescu, A.M., Nardou, F., Zichil, V., Nistor, I.D., 2018. Adsorption of lead(II) ions from aqueous solutions onto Cr-pillared clays. Appl. Clay Sci. 152, 44–50.
Geselnikova, O., Barras, A., Addad, A., Sviridova, E., Szunerits, S., Postnikov, P., Boukherroub, R., 2020. Magnetic polyurethane sponge for efficient oil adsorption and separation of oil from oil-in-water emulsions. Sep. Purif. Technol. 240, 116627.
Guselnikova, O., Barras, A., Addad, A., Sviridova, E., Szunerits, S., Postnikova, P., Boukherroub, R., 2020. Magnetic polyurethane sponge for efficient oil adsorption and separation of oil from oil-in-water emulsions. Sep. Purif. Technol. 240, 116627.
Gupta, V.K., Ali, I. Saleh, Nayak, T.A., Agarwal S., A., 2012. Chemical treatment technologies for waste-water recycling. RSC Adv. 2, 6380–6388.
Gwenzi, W., Chaukura, N., 2018. Organic Contaminants in African Aquatic Systems: Current Knowledge, Health Risks, and Future Research Directions. Sci. Total Environ. (619-620), 1493–1514. https://doi.org/10.1016/j.scitotenv.2017.11121.
Gwenzi, W., Musiyiwa, K., Mangori, L., 2020. Sources, behaviour and health risks of antimicrobial resistance genes in wastewaters: a hotspot reservoir. J. Environ. Chem. Eng. 8 (1), 102220.
Hanandeh, A.E., Mahdi, Z., Imtiaz, M.S., 2021. Modelling of the Adsorption of Pb, Cu and Ni ions from single and multi-component aqueous solutions by date seed derived biochar: comparison of six machine learning approaches. Environ. Res. 192, 110338 https://doi.org/10.1016/j.envres.2020.110338.
Hanieh, N., Samira, F., Sheida, Z., Seyed Heydar, M.M., Neda, A.K., Seyedmehdi, S., 2021. A comprehensive study on modified-pillared clays as an adsorbent in wastewater treatment processes. Process Saf. Environ. Prot. 147, 8–36.
Hariharan, A., Harini, V., Sandhya, Sai, Rangabhashiyam, S., 2020. Waste Musa acuminata residue as a potential biosorbent for the removal of hexavalent chromium from synthetic wastewater. Biomass Convers. Biorefin. https://doi.org/10.1007/s13399-020-01173-3.
Hong, H.-J., Lim, J.S., Hwang, J.Y., Kim, M., Jeong, H.S., Park, M.S., 2018. Carboxymethlyated cellulose nanofibrils(CMCNFs) embedded in polyurethane foam as a modular adsorbent of heavy metal ions. Carbohydr. Polym. 195, 136–142.
Hugo, O.V., Nissim, G.D., Orlando, G.R., Srikanth, M., Olivier, L., 2021. Electro-Fenton treatment of real pharmaceutical wastewater paired with a BDD anode: reaction mechanisms and respective contribution of homogeneous and heterogeneous OH. Chem. Eng. J. 404, 126524.
Hussein, F.B., Abu-Zahra, N.H., 2016. Synthesis, characterization and performance of polyurethane foam nanocomposite for arsenic removal from drinking water. J. Water Process Eng. 13, 1–5.
Igberase, E., Osifo, P.O., 2019. Mathematical modelling and simulation of packed bed column for the efficient adsorption of Cu(II) ions using modified bio-polymeric material. J. Environ. Chem. Eng. 7, 103129.

Iman, A.S., Nabil, Z., Mohammad, A.A.G., 2020. Removal of pesticides from water and wastewater: chemical, physical and biological treatment approaches. Environ. Technol. Innov. 19, 101026.
Jamsaz, A., Goharshadi, E.K., 2020. An environmentally friendly superhydrophobic modified polyurethane sponge by seashell for the efficient oil/water separation. Process Saf. Environ. Prot. 139, 297–304.
Jessica, B., Emmanuel, S., Renald, B., 2020. Heavy metal pollution in the environment and their toxicological effects on humans. Heliyon 6, e04691.
Jin, L., Gao, Y., Yin, J., Zhang, X., He, C., Wei, Q., Liu, X., Liang, F., Zhao, W., Zhao, C., 2020. Functionalized polyurethane sponge based on dopamine derivative for facile and instantaneous clean-up of cationic dyes in a large scale. J. Hazard. Mater. 400, 123203.
Kalaivani, S.S., Muthukrishnaraj, A., Sivanesan, S., Ravikumar, L., 2016. Novel hyperbranched polyurethane resins for the removal of heavy metal ions from aqueous solution. Process Saf. Environ. Prot. 104, 11–23.
Kaljurand, I., Kütt, A., Sooväli, L., Rodima, T., Mäemets, V., Leito, I., Koppel, I.A., 2005. Extension of the self-consistent spectrophotometric basicity scale in acetonitrile to a full span of 28 pKa units: unification of different basicity scales. J. Org. Chem. 70 (3), 1019–1028.
Kaljurand, I., Rodima, T., Leito, I., Koppel, I.A., Schwesinger, R., 2000. Self-consistent spectrophotometric basicity scale in acetonitrile covering the range between pyridine and DBU. J. Org. Chem. 65 (19), 6202–6208.
Karimi-Maleh, H., Ayati, A., Davoodi, R., Tanhaei, B., Karimi, F., Malekmohammadi, S., Orooji, Y., Fu, L., Sillanpää, M., 2021. Recent advances in using of chitosan-based adsorbents for removal of pharmaceutical contaminants: a review. J. Clean. Prod. 291, 125880.
Khademian, E., Salehi, E., Sanaeepur, H., Galiano, F., Figoli, A., 2020. A systematic review on carbohydrate biopolymers for adsorptive remediation of copper ions from aqueous environments—Part B: isotherms, thermokinetics and reusability. Sci. Total Environ., 142048
Khalilifard, M., Javadian, S., 2020. Magnetic superhydrophobic polyurethane sponge loaded with Fe3O4@oleic acid@graphene as high performance adsorbent oil from water. Chem. Eng. J. 127369, 1385–8947. https://doi.org/10.1016/j.cej.2020.127369.
Khan, F.S.A., Mubarak, N.M., Tan, Y.H., Khalid, M., Karri, R.R., Walvekar, R., Abdullah, E.C., Nizamuddin, S., Mazari, S.A., 2021. A comprehensive review on magnetic carbon nanotubes and carbon nanotube-based buckypaper-heavy metal and dyes removal. J. Hazard. Mater. 125375.
Khan, T.A., Nazir, M., Khan, E.A., Riaz, U., 2015. Multiwalled carbon nanotube-polyurethane (MWCNT/PU) composite adsorbent for safranin T and Pb(II) removal from aqueous solution: batch and fixed-bed studies. J. Mol. Liq. 212, 467–479.
Khalid, M.Z., Haq, N.B., Ijaz, A.B., 2007. Methods for polyurethane and polyurethane composites, recycling and recovery: a review. React. Funct. Polym. 67, 675–692.
Kong, L., Qiu, F., Zhao, Z., Zhang, X., Zhang, T., Pan, J., Yang, D., 2016. Removal of brilliant green from aqueous solutions based on polyurethane foam adsorbent modified with coal. J. Clean. Prod. 137, 51–59.
Kumari, S., Chauhan, G.S., Ahn, J.-H., 2016. Novel cellulose nanowhiskers-based polyurethane foam for rapid and persistent removal of methylene blue from its aqueous solutions. Chem. Eng. J. 304, 728–736.
Kupeta, A.J.K., Naidoo, E.B., Ofomaja, A.E., 2018. Kinetics and equilibrium study of 2-notrophenol adsorption onto polyurethane cross-linked pine cone biomass. J. Clean. Prod. 179, 191–209.
Kütt, A., Rodima, T., Saame, J., Raamat, E., Mäemets, V., Kaljurand, I., Koppel, I.A., Garlyauskayte, R.Y., Yagupolskii, Y.L., Yagupolskii, L.M., Bernhardt, E., Willner, H., Leito, I., 2010. Equilibrium acidities of superacids. J. Org. Chem. 76 (2), 391–395.
Larissa, S.M., Francisco, M.M., Daniella, R.M., 2020. Influence of the granulometry and fiber content of palm residues on the diesel S-10 oil sorption in polyurethane /palm fiber biocomposites. Results Mater. 8, 100143.
Lefebvre, L., Kelber, J., Jierry, L., Ritleng, V., Edouard, D., 2017. Polydopamine-coated open cell polyurethane foam as an efficient and easy-to-regenerate soft structured catalytic support (S2CS) for the reduction of dye. J. Environ. Chem. Eng. 5, 79–85.
Lefebvre, L., Agusti, G., Bouzeggane, A., Edouard, D., 2018. Adsorption of dye with carbon media supported on polyurethane open cell foam. Catal. Today 301, 98–103.
Leudjo Taka, A., Fosso-Kankeu, E., Pillay, K., Yangkou Mbianda, X., 2020. Metal nanoparticles decorated phosphorylated carbon nanotube/ cyclodextrin nanosponge for trichloroethylene and Congo red dye adsorption from wastewater. J. Environ. Chem. Eng. 8, 103602.
Leudjo Taka, A., Pillay, K., Mbianda, X.Y., 2018. Synthesis and characterization of a novel bio nanosponge filter (pMWCNT-CD/TiO2-Ag) as potential adsorbent for water purification. In: Ramasami, P., Bhowon, M.G., Laulloo, S.J., Li, H., Wah, K. (Eds.), Emerging Trends in Chemical Sciences. Springer International Publishing AG, pp. 313–343.
Li, X., Nie, X.-J., Zhu, Y.-N., Ye, W.-C., Jiang, Y.-L., Su, S.-L., Yan, B.-T., 2019. Adsorption behaviour of Eriochrome Black T from water onto a cross-linked β-cyclodextrin polymer. Colloids Surf. A Physicochem. Eng. Asp. 578, 123582.
Li, Z., Chen, K., Li, W., Biney, B.W., Guo, A., 2020. Removal of malachite green dye from aqueous solution by adsorbents derived from polyurethane plastic waste. J. Environ. Chem. Eng., 104704 https://doi.org/10.1016/j.jece.2020.104704.
Lin, C., Fan, Y., Guihong, G., Minda, R., Jiachen, S., Le, T., 2019. The use of polyurethane for asphalt pavement engineering applications: a state-of-the-art review. Constr. Build. Mater. 225, 1012–1025.
Lu, T., Yu, D., Chen, G., Wang, X., Huang, S., Liu, C., Tang, P., 2019. NH4+-N adsorption behavior of nitrifying sludge immobilized in waterborne polyurethane (WPU) pellets. Biochem. Eng. J. 143, 196–201.
Lyu, S., Grailer, T., Belu, A., Schley, J., Bartlett, T., Hobot, C., Sparer, R., Untereker, D., 2007. Nano-adsorbents control surface properties of polyurethane. Polymer 48, 6049–6055.
Magdalena, C.S., Marieta, N., 2018. Influence of dextran hydrogel characteristics on adsorption capacity for anionic dyes. Carbohydr. Polym. 199, 75–83.
Mahak, J., Abhradeep, M., Partha, S.G., Ashok, K.G., 2020. A review on treatment of petroleum refinery and petrochemical plant wastewater: a special emphasis on constructed wetlands. J. Environ. Manag. 272, 111057.
Maaloul, N., Oulego, P., Rendueles, M., Ghorbal, A., Díaz, M., 2021. Biopolymer composite from cellulose nanocrystals of almond (Prunus dulcis) shell as effective adsorbents for Cu2+ ions from aqueous solutions. J. Environ. Chem. Eng. 9 (2), 105139.
Mamba, G., Mbianda, X.Y., Govender, P.P., 2013. Phosphorylated multiwalled carbon nanotube-cyclodextrin polymer: synthesis, characterisation and potential application in water purification. Carbohydr. Polym. 98, 470–476.
Manjunath, S.V., Kumar, M., 2018. Evaluation of single-component and multi-component adsorption of metronidazole, phosphate and nitrate on activated carbon from Prosopıs julıflora. Chem. Eng. J. 346, 525–534.
Mangaleshwaran, L., Thirulogachandar, A., Rajasekar, V., Muthukumaran, C., Rasappan, K., 2015. Batch and fixed bed column studies on nickel (II) adsorption from aqueous solution by treated polyurethane foam. J. Taiwan Inst. Chem. Eng. 55, 112–118.
Marlina, Iqhrammullah, M., Saleha, S., Fathurrahmi, Maulina, F.P., Idroes, R., 2020. Polyurethane film prepared from ball-milled algal polyol particle and activated carbon filler for NH3-N removal. Heliyon 6, 04590.
Martins, L.S., Monticelli, F.M., Mulinari, D.R., 2020. Influence of the granulometry and fiber content of palm residues on the diesel S-10 oil sorption in polyurethane/palm fiber biocomposites. Results Mater. 8, 100143.
Maryam, H., Mohammad, H., 2020. Application of three dimensional porous aerogels as adsorbent for removal of heavy metal ions from water/wastewater: a review study. Adv. Colloid Interface Sci. 284, 102247.
Mendieta-Rodríguez, L.S., González-Rodríguez, L.M., Alcaraz-Espinoza, J.J., Chávez-Guajardo, A.E., Medina-Llamas, J.C., 2021. Synthesis and characterization of a polyurethane-polyaniline macroporous foam material for methyl orange removal in aqueous media. Mater. Today Commun. 26, 102155.
Mhlanga, S.D., Mamba, B.B., Krause, R.W., Malefetse, T.J., 2007. Removal of organic contaminants from water using nanosponge cyclodextrin polyurethanes. Journal of Chemical Technology & Biotechnology: International Research in Process. Environ. Clean Techno. 82 (4), 382–388.
Misbah, S., Khalid, M.Z., Haq, N.B., Tahir, J., Rizwan, H., Mohammad, Z., 2012. Modification of cellulosic fiber with polyurethane acrylate copolymers. Part I: physicochemical properties. Carbohydr. Polym. 87, 397–404.
Moawed, E.A., Abulkibash, A.B., El-Shahat, M.F., 2015. Synthesis and characterization of iodo polyurethane foam and its application in removing of aniline blue and crystal violet from laundry wastewater. J. Taibah Uni. Sci. 9 (1), 80–88.
Moawed, E.A., Radwan, A.M., 2017. Application of acid modified polyurethane foam surface for detection and removing of organochlorine pesticides from wastewater. J. Chromatography B 1044, 95–102.
Mohammadi, A., Lakouraj, M.M., Barikani, M., 2014. Preparation and characterization of p-tert-butyl thiacalix [4] arene imbedded flexible polyurethane foam: an efficient novel cationic dye adsorbent. React. Funct. Polym. 83, 14–23.
Mojerlou, F., Lakouraj, M.M., Barikani, M., Mohammadi, A., 2019. Highly efficient polyurethane membrane based on nanocomposite of sulfonated thiacalix[4]arene-sodium alginate for desalination. Carbohydr. Polym. 205, 353–361.
Moreira, F.C., Soler, J., Alpendurad, M.F., Boaventura, Rui A.R., Brillas, Enric, Vilar, V. ítor J.P., 2016. Tertiary treatment of a municipal wastewater toward pharmaceuticals removal by chemical and electrochemical advanced oxidation processes. Water Res. 105, 251–263.
Morin-Crini, N., Crini, G., 2013. Environmental applications of water-insoluble β-cyclodextrin–epichlorohydrin polymers. Prog. Polym. Sci. 38, 344–368.
Mustapha, S., Ndamitso, M.M., Abdulkareem, A.S., Tijani, J.O., Mohammed, A.K., Shuaib, D.T., 2019. Potential of using kaolin as a natural adsorbent for the removal of pollutants from tannery wastewater. Heliyon 5, e02923.
Narayanan, N., Gupta, S., Gajbhiye, V.T., 2020. Decontamination of pesticide industrial effluent by adsorption–coagulation–flocculation process using biopolymer-nanoorganoclay composite. Int. J. Environ. Sci. Technol. 17, 4775–4786.
Nasiri, S., Alizadeh, N., 2019. Synthesis and adsorption behavior of hydroxypropyl β-cyclodextrin–polyurethane magnetic nanoconjugates for crystal and methyl violet dyes removal from aqueous solutions. RSC Adv. 9, 24603–24616.
Neta, J.J.S., Moreira, G.C., da Silva, C.J., Reis, C., Reis, E.L., 2011. Use of polyurethane foams for the removal of the Direct Red 80 and Reactive Blue 21 dyes in aqueous medium. Desalination 281, 55–60.
Nethaji, S., Tamilarasan, G., Neehar, P., Sivasamy, A., 2018. Visible light photocatalytic activities of BiOBr-activated carbon (derived from waste polyurethane) composites by hydrothermal process. J. Environ. Chem. Eng. 6, 3735–3744.
Nikkhah, A.A., Zilouei, H., Asadinezhad, A., Keshavarz, A., 2015. Removal of oil from water using polyurethane foam modified with nanoclay. Chem. Eng. J. 262, 278–285.
Noorisafa, Fatemeh, Razmjou, Amir, Emami, Nahid, Low, Ze-Xian, Korayem, Asghar Habibnejad, Kajani, Abolghasem Abbasi, 2016. Surface modification of polyurethane via creating a biocompatible superhydrophilic nanostructured layer: role of surface chemistry and structure. J. Exp. Nanosci. 11 (14), 1087–1109. https://doi.org/10.1080/17458080.2016.1188223.
Okoli, C.P., Adewuyi, G.O., Zhanga, Q., Diagboya, P.N., Guo, Q., 2014. Mechanism of dialkyl phthalates removal from aqueous solution using γ-cyclodextrin and starch based polyurethane polymer adsorbents. Carbohydr. Polym. 114, 440–449.

Paci, E., 2012. Using models to design new bioinspired materials. Biophys. J. 103 (9), 1814–1815.
Peng, X., Mo, S., Li, R., Li, J., Tian, C., Liu, W., Wang, Y., 2021. Effective removal of the rare earth element dysprosium from wastewater with polyurethane sponge-supported graphene oxide–titanium phosphate. Environ. Chem. Letters 19 (1), 719–728.
Pinto, M.L., Pires, J., Carvalho, A.P., de Carvalho, M.B., Bordado, J.C., 2005. Characterization of adsorbent materials supported on polyurethane foams by nitrogen and toluene adsorption. Microporous Mesoporous Mater. 80, 253–262.
Qin, H., Wang, H., 2019. Study on preparation and performance of PEG-based polyurethane foams modified by the chitosan with different molecular weight. Int. J. Biol. Macromol. 140, 877–885.
Quek, E., Ting, Y.P., Tan, H.M., 2006. Rhodococcus sp. F92 immobilized on polyurethane foam shows ability to degrade various petroleum products. Biores. Tech. 97 (1), 32–38.
Quintiles IMS, 2015. Global Medicines Use in 2020, Outlook Implic, pp. 9–21.
Ramazanova, G.R., Tikhomirova, T.I., Apyari, V.V., 2013. Sorption of food dyes on polyurethane foam and aluminum oxide. Moscow University Chemistry Bulletin 68 (4), 175–180.
Radha, G., Sunil, K.G., Devendra DP, D.P., 2019. Selective adsorption of toxic heavy metal ions using guanine-functionalized mesoporous silica [SBA-16-g] from aqueous solution. Microporous Mesoporous Mater. 288, 109577.
Rangabhashiyam, S., Vijayaraghavan, K., 2019. Biosorption of Tm(III) by free and polysulfone-immobilized Turbinaria conoides biomass. J. Ind. Eng. Chem. 80, 318–324.
Rangabhashiyam, S., Giri Nandagopal, M.S., Nakkeeran, E., Selvaraju, N., 2016. Adsorption of hexavalent chromium from synthetic and electroplating effluent on chemically modified Swietenia mahagoni shell in a packed bed column. Environ. Monit. Assess. 188, 411.
Rangabhashiyam, S., Balasubramanian, P., 2018. Adsorption behaviors of hazardous methylene blue and hexavalent chromium on novel materials derived from Pterospermum acerifolium shells. J. Mol. Liq. 254, 433–445.
Rangabhashiyam, S., Balasubramanian, P., 2019. The potential of lignocellulosic biomass precursors for biochar production: performance, mechanism and wastewater application—A review. Ind. Crops Prod. 128, 405–423.
Ranote, S., Kumar, D., Kumari, S., Kumar, R., Chauhan, G.S., Joshi, V., 2019. Green synthesis of Moringa oleifera gum-based bifunctional polyurethane foam braced with ash for rapid and efficient dye removal. Chem. Eng. J. 361, 1586–1596.
Raphael, J., Mrinal, K.M., Kashyap, K.D., Patricia, L., 2017. Slurry photocatalytic membrane reactor technology for removal of pharmaceutical compounds from wastewater: towards cytostatic drug elimination. Sci. Total Environ. 599–600, 612–626.
Raspoet, G., Nguyen, M.T., McGarraghy, M., Hegarty, A.F., 1998. Experimental and theoretical evidence for a concerted catalysis by water clusters in the hydrolysis of isocyanates. J. Org. Chem. 63 (20), 6867–6877.
Saad, H.A., Natheer, N.I., Ali, D.A., Wisam, M.A., 2019. Electrocoagulation technique for refinery wastewater treatment in an internal loop split-plate airlift reactor. J. Environ. Chem. Eng. 7, 103489.
Salipira, K.L., Krause, R.W., Mamba, B.B., Malefetse, T.J., Cele, L.M., Durbach, S.H., 2008. Cyclodextrin polyurethanes polymerised with multiwalled carbon nanotubes: synthesis and characterisation. Mater. Chem. Phys. 111, 218–224.
Salipira, K.L., Mamba, B.B., Krause, R.W., Malefetse, T.J., Durbach, S.H., 2008. Cyclodextrin polyurethanes polymerised with carbon nanotubes for the removal of organic pollutants in water. Water SA 34 (1), 113–118.
Santos, O.S.H., Mercês Coelho da Silva, V.R., Silva, W.N., Mussel, M.I., Yoshida, 2017. Polyurethane foam impregnated with lignin as a filler for the removal of crude oil from contaminated water. J. Hazard. Mater. 324, 406–413.
Saranya, M., Latha, S., Gopal Reddi, M.R., Gomathi, T., Sudha, P.N., Anil, S., 2017. Adsorption studies of lead(II) from aqueous solution onto nanochitosan/ polyurethane/ polypropylene glycol ternary blends. Int. J. Biol. Macromol. 104, 1436–1448.
Sardon, H., Engler, A.C., Chan, J.M.W., García, J.M., Coady, D.J., Pascual, A., Mecerreyes, D., Jones, G.O., Rice, J.E., Horn, H.W., Hedrick, J.L., 2013. Organic acid-catalyzed polyurethane formation via a dual-activated mechanism: unexpected preference of n-activation over o-activation of isocyanates. J. Am. Chem. Soc. 135, 16235–16241.
Sarita, D., Rahul, K., Akash, D., Mayur, B.K., Sang-Woo, J., Byong-Hun, J., 2019. Metal–organic frameworks (MOFs) for the removal of emerging contaminants from aquatic environments. Coord. Chem. Rev. 380, 330–352.
Sarode, S., Upadhyay, P., Khosa, M.A., Mak, T., Shakir, A., Song, S, A., 2019. Overview of wastewater treatment methods with special focus on biopolymer chitinchitosan. Int. J. Biol. Macromol. 121, 1086–1100.
Selvakumar, A., Rangabhashiyam, S., 2019. Biosorption of Rhodamine B onto novel biosorbents from Kappaphycus alvarezii, Gracilaria salicornia and Gracilaria edulis. Environ. Pollut. 255, 113291.
Simon, D., Borreguero, A.M., de Lucas, A., Rodríguez, J.F., 2018. Recycling of polyurethanes from laboratory to industry, a journey towards the sustainability. Waste Manag. 76, 147–171.
Sone, H., Fugetsu, B., Tanaka, S., 2009. Selective elimination of lead(II) ions by alginate/ polyurethane composite foams. J. Hazard. Mater. 162, 423–429.
Sonnenschein, M.F., Wendt, B.L., 2013. Design and formulation of soybean oil derived flexible polyurethane foams and their underlying polymer structure/property relationships. Polymer 54 (10), 2511–2520.
Subramanian, N., Hari, C.B., Rajesh, J.T., 2018. Recent advances based on the synergetic effect of adsorption for removal of dyes from waste water using photocatalytic process. J. Environ. Sci. 65, 201–222.
Sultan, M., Islam, A., Gul, N., Bhatti, H.N., Safa, Y., 2015. Structural variation in soft segment of waterborne polyurethane acrylate nanoemulsions. J. Appl. Polym. Sci. 132, 41706.
Sultan, M., Javeed, A., Uroos, M., Imran, M., Jubeen, F., Nouren, S., Saleem, N., Bibi, I., Masood, R., Ahmed, W., 2018. Linear and crosslinked polyurethanes based catalysts for reduction of methylene blue. J. Hazard. Mater. 344, 210–219.
Taka, A.L., Pillay, K., Mbianda, X.Y., 2017. Nanosponge cyclodextrin polyurethanes and their modification with nanomaterials for the removal of pollutants from waste water: A review. Carbohydrate Polymers 159, 94–107.
Tahir, R., Adeel, A.H., Muhamad, B., Tariq, H., Komal, R., 2020. Metal-organic frameworks based adsorbents: a review from removal perspective of various environmental contaminants from wastewater. Chemosphere 259, 127369.
Tan, X., Liu, Y., Gu, Y., Liu, S., Zeng, G., Cai, X., Hu, X., Wang, H., Liu, S., Jiang, L., 2016. Biochar pyrolyzed from MgAl-layered double hydroxides pre-coated ramie biomass (Boehmeria nivea (L.) gaud.): characterization and application for crystal violet removal. J. Environ. Manag. 184, 85–93.
Tikhomirova, T.I., Ramazanova, G.R., Apyari, V.V., 2018. Effect of nature and structure of synthetic anionic food dyes on their sorption onto different sorbents: Peculiarities and prospects. Microchem. J. 143, 305–311.
Torres, C.I., Ramakrishna, S., Chiu, C.A., Nelson, K.G., Westerhoff, P., Krajmalnik-Brown, R., 2011. Fate of sucralose during wastewater treatment. Environ. Eng. Sci. 28, 325–331.
Tran, H.N., You, S.J., Hosseini-Bandegharaei, A., Chao, H.P., 2017. Mistakes and inconsistencies regarding adsorption of contaminants from aqueous solutions: a critical review. Water Res. 120, 88–116.
Travieso, L., Canizares, R.O., Borja, R., Benitez, F., Dominguez, A.R., Valiente, V., 1999. Heavy metal removal by microalgae. Bulletin Environ. Contamination Toxicol. 62 (2), 144–151.
United Nations, Department of economic and Social Affairs, Population Division, 2011. World Population Prospects: the 2010 Revision, Highlights and Advance Tables. ESA/P/WP.220.
Vafaeifard, M., Ibrahim, S., Wong, K.T., Pasbakhsh, P., Pichiah, S., Choi, J., Yoon, Y., Jang, M., 2019. Novel self-assembled 3D flower-like magnesium hydroxide coated granular polyurethane: implication of its potential application for the removal of heavy metals. J. Clean. Prod. 216, 495–503.
Vali, S.A., Baghdadi, M., Abdoli, M.A., 2018. Immobilization of polyaniline nanoparticles on the polyurethane foam derived from waste materials: a porous reactive fixed-bed medium for removal of mercury from contaminated waters. J. Environ. Chem. Eng. 6, 6612–6622.
Vikash, S., Vimal, C.S., 2020. Self-engineered iron oxide nanoparticle incorporated on mesoporous biochar derived from textile mill sludge for the removal of an emerging pharmaceutical pollutant. Environ. Pollut. 259, 113822.
Vinhal, J.O., Nege, K.K., Lage, M.R., Carneiro, J.W.M., Lima, C.F., Cassella, R.J., 2017. Adsorption of the herbicides diquat and difenzoquat on polyurethane foam: Kinetic, equilibrium and computational studies. Ecotoxicol. Environ. Safety 145, 597–604.
Vintu, M., Unnikrishnan, G., 2019. Indolocarbazole based polymer coated super adsorbent polyurethane sponges for oil/organic solvent removal. J. Environ. Manag. 248, 109344.
Viraj, G., Anushka, U.R., Meththika, V., Daniel, S.A., Rangabhashiyam, S., Naushad, Mu, Siming, Y., Patryk, O., Ok, Yong Sik, 2020. Hydrometallurgical processes for heavy metals recovery from industrial sludges. Crit. Rev. Environ. Sci. Technol. https://doi.org/10.1080/10643389.2020.1847949.
Waletzko, R.S., Korley, L.S.T.J., Pate, B.D., Thomas, E.L., Hammond, P.T., 2009. Role of increased crystallinity in deformation-induced structure of segmented thermoplastic polyurethane elastomers with PEO and PEO-PPO-PEO soft segments and HDI hard segments. Macromolecules 42, 2041–2053.
Xie, D., Howard, L., Almousa, R., 2018. Surface modification of polyurethane with a hydrophilic, antibacterial polymer for improved antifouling and antibacterial function. J. Biomater. Appl. 33 (3), 340–351. https://doi.org/10.1177/0885328218792687.
Xin, L., Min, J., Long, D.N., Yingxin, Z., Duo, L., Ying, Y., Qian, W., Quang, T.T., Dai-Viet, N.V., Van, Q.P., Ngoc, H.T., 2020. A novel red mud adsorbent for phosphorus and diclofenac removal from wastewater. J. Mol. Liq. 303, 112286.
Xue, D., Li, T., Liu, Y., Yang, Y., Zhang, Y., Cui, J., Guo, D., 2019. Selective adsorption and recovery of precious metal ions from water and metallurgical slag by brush graphene-polyurethane composite. React. Funct. Polym. 136, 138–152.
Yang, H.-C., Gong, J.-, Zeng, G.-M., Zhang, P., Zhang, J., Liu, H.-Y., Huan, S.-Y., 2017. Polyurethane foam membranes filled with humic acid-chitosan crosslinked gels for selective and simultaneous removal of dyes. J. Colloid Interface Sci. 505, 67–78.
Yang, X., Wang, J.-N., Cheng, C., 2013. Preparation of new spongy adsorbent for removal of EDTA-Cu(II) and EDTA-Ni(II) from water. Chin. Chem. Lett. 24, 383–385.
Yu, H., Zhu, Y., Xu, J., Wang, A., 2020a. Fabrication porous adsorbents templated from modified sepiolite-stabilized aqueous foams for high-efficient removal of cationic dyes. Chemosphere 259, 126949.
Yu, Z., Leng, H., Luo, Q., Zhang, J., Wu, X., Chou, K.-C., 2020b. New insights into ternary geometrical models for material design. Mater. Des. 192, 108778.
Yuling, T., Jieting, Z., Yingjiao, Z., Jianfei, Z., Bi, S., 2021. Conversion of tannery solid waste to an adsorbent for high-efficiency dye removal from tannery wastewater: a road to circular utilization. Chemosphere 263, 127987.
Zahra, S., Ali, P., 2019. Recent advances on pollutants removal by rice husk as a bio-based adsorbent: a critical review. J. Environ. Manag. 246 (15), 314–323.
Zeng, Z.W., Tan, X.F., Liu, Y.G., Tian, S.R., Zeng, G.M., Jiang, L.H., Liu, S.B., Li, J., Liu, N., Yin, Z.H., 2018. Comprehensive adsorption studies of doxycycline and ciprofloxacin antibiotics by biochars prepared at different temperatures. Front. Chem. 6, 80.

Zenoozi, S., Sadeghi, G.M.M., Rafiee, M., 2020. Synthesis and characterization of biocompatible semi-interpenetrating polymer networks based on polyurethane and cross-linked poly (acrylic acid). Eur. Polym. J. 140, 109974.

Zhou, L.C., Li, Y.F., Bai, X., Zhao, G.H., 2009. Use of microorganisms immobilized on composite polyurethane foam to remove Cu (II) from aqueous solution. J. Hazardous Mater. 167 (1-3), 1106–1113.

Zhuang, Y.T., Gao, W., Yu, Y., Wang, J., 2016. A three-dimensional magnetic carbon framework derived from Prussian blue and amylopectin impregnated polyurethane sponge for lead removal. Carbon 108, 190–198.

Zia, K.M., Bhatti, H.N., Bhatti, I.A., 2007. Methods for polyurethane and polyurethane composites, recycling and recovery: a review. React. Funct. Polym. 67, 675–692.

Zia, F., Zia, K.M., Zuber, M., Kamal, S., Aslam, N., 2015. Starch based polyurethanes: a critical review updating recent literature. Carbohydr. Polym. 134, 784–798.

Zonoozi, M.H., Alavi Moghaddam, M.R., Maknoon, R., 2015. Operation of integrated sequencing batch membrane bioreactor treating dye-containing wastewater at different SRTs: study of overall performance and fouling behavior. Environ. Sci. Pollut. Res. 22, 5931–5942.